ChemistrySelect

Review
doi.org/10.1002/slct.202401265

Chemistry Europe
European Chemical Societies Publishing

www.chemistryselect.org

Advances in Plasmonic Photonic Crystal Fiber Biosensors: Exploring Innovative Materials for Bioimaging and Environmental Monitoring

Sareh Vatani[+],[a] Jeshurun Biney[+],[a] Vahid Faramarzi[+],[b] Ghassan Jabbour,[c] and Jeongwon Park*[a, c]

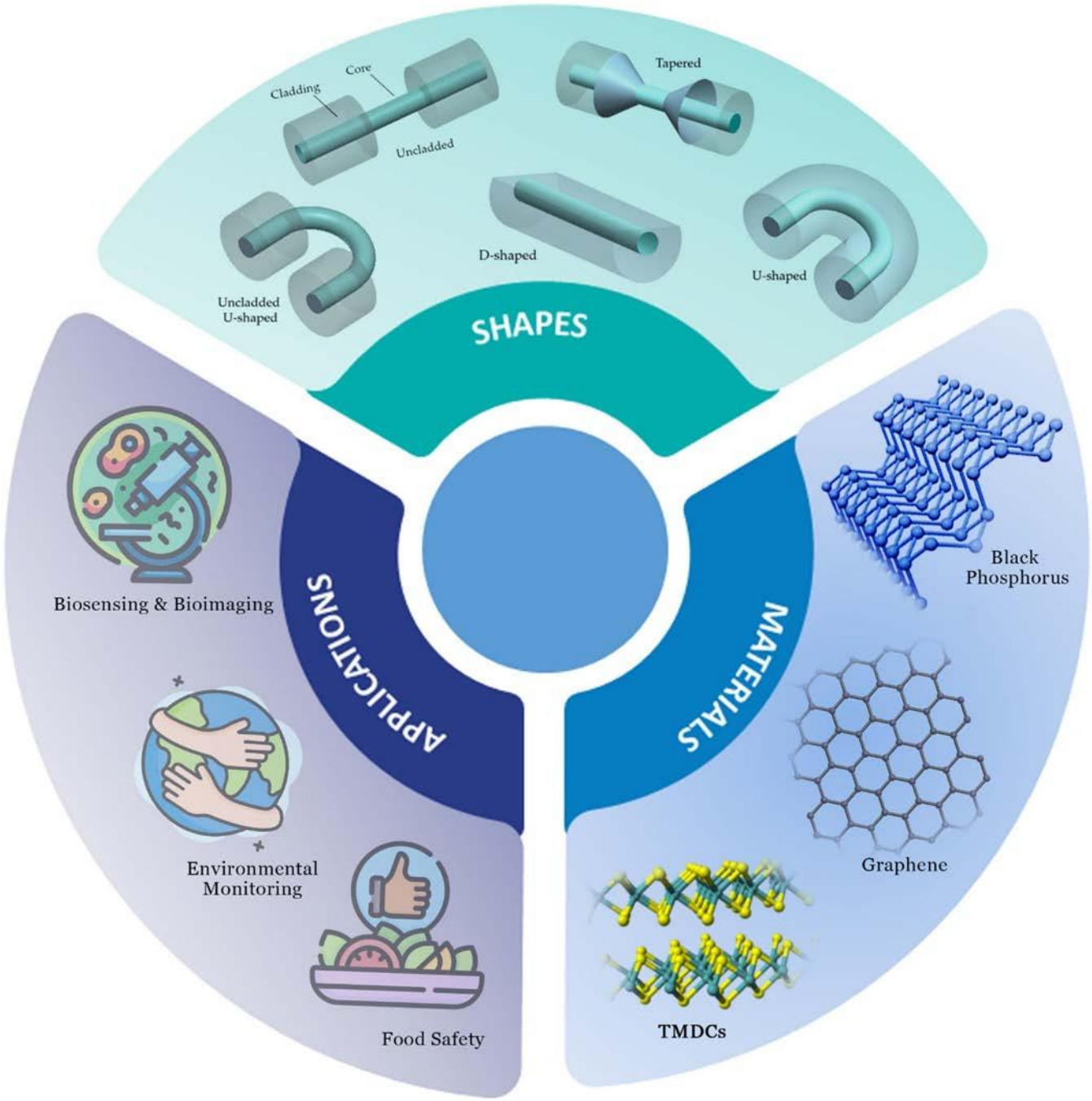

This review paper comprehensively analyzes recent advancements in optical fiber-based biosensors, focusing on conventional fiber and photonic crystal structures. This paper overviews the significant applications of optical fiber biosensors, including bioimaging, quality analysis, food safety, and field environment monitoring, setting the stage for subsequent discussions. The primary objective of the review is to systematically evaluate recent literature concerning optical fiber-based biosensors, emphasizing their sensitivities and resolutions. The second section explores integrating plasmonic materials such as graphene, TDMC, germanium, black phosphorus, and silicon within optical fiber biosensors, elucidating their roles in enhancing sensitivity and resolution in biosensing applications. A detailed examination of photonic crystal fibers (PCF) follows, categorizing them into internally and externally metal film-coated biosensors, highlighting their distinct advantages and limitations. Comparative analyses in two tables delineate the performance and sensitivity of optical fiber-based biosensors, mainly focusing on different coating strategies. The final section of the review discusses emerging trends and applications in optical fiber biosensing technologies, underscoring their potential to transform biomedical and environmental monitoring fields. By synthesizing recent developments and challenges, this review aims to offer researchers and practitioners a comprehensive understanding of optical fiber-based biosensors, facilitating informed decision-making and driving further advancements in the field.

1. Introduction

Biosensors represent compact analytical devices that integrate a biological sensing element with electrical, optical, or chemical transducers. Significant advancements have transformed biosensors' functionality, design, and fabrication in recent decades. Introducing new materials, flexible fabrication technology, and continuing developments in fabrication techniques have played vital roles in this evolution.[1,2] In managing infections, early diagnosis is crucial for reducing mortality rates. This underscores the importance of biosensors and their significant role in medicine and society.[3] Label-free optical detection methods are of great interest for biosensing and single-cell investigations. These methods avoid the time-consuming and costly biomolecular labeling and enable the elucidation of molecular interactions in a noninvasive and dynamic approach.[4] In particular, the SPR methods hold great promise for biosensing and bioimaging because of their compatibility with physiological solutions, robust performance, and ability to real-time quantification of biomolecule interactions.[5,6] SPRs are collective oscillations of free electrons propagating at the interface between a dielectric and a conductor.[7] These phenomena occur through the coupling of photons and electrons.[8]

SPR biosensors use plasmonic waves to probe the interactions between biomolecules and the sensor surface. As SPRs confine the optical energy of light into the subwavelength scale, they are very sensitive to slight changes in the refractive index (RI) of the environmental medium.[9] Owing to their compact structure, high sensitivity, and real-time monitoring of biomolecules, SPR-based biosensors, numerous applications have been suggested for these phenomena across diverse fields, encompassing biology, and immunosensors,[10,11] food safety,[12,13] environmental monitoring,[14,15] gas sensing,[16,17] image sensing,[18,19] and optical communication.[20,21] SPR-based sensors have emerged as indispensable tools in biosensing, exhibiting a remarkable capability to detect minute changes in the RI of sensing materials within their environment. This heightened sensitivity has propelled their prominence in biosensing applications, capitalizing on the specific RI values exhibited by various biomaterials, liquid analytes, and gases, including different cancerous cells and blood components. Exploiting this distinctive feature facilitates the convenient detection of RI changes, opening avenues for high-sensitivity detection across various applications. Noteworthy examples include the detection of various diseases, blood components,[22] biological molecules,[23] DNA-related phenomena,[24] cancerous cells,[25] viruses,[26,27] bacteria,[28] as well as the quantification of protein and glucose concentrations in human urine.[29,30]

In the landscape of biosensor research, the application of advanced materials like graphene,[31] black phosphorous,[32] silicon,[33] germanium,[34] and transition metal dichalcogenides (TMDC)[35] has garnered significant attention. This review delves into plasmonic biosensors, examining their incorporation into diverse structures such as conventional optical fiber and PCF. By exploring the unique properties of these materials, this paper aims to provide insights into the evolving landscape of biosensor technology. Incorporating innovative materials and distinct sensor structures enriches our understanding of plasmonic biosensors and holds promise for enhancing their efficiency and applicability in various analytical and diagnostic domains.

When the frequency of incident photons resembles that of the surface electrons of the conductor (plasmonic material), the p-polarized light excites mobile charge carriers (free electrons) of the conductor surface. Thus, the incident light is absorbed by the free electrons of the conductor surface, and a surface plasmon wave in the form of collective oscillations is generated

[a] S. Vatani,[+] J. Biney,[+] J. Park
Electrical & Biomedical Engineering, University of Nevada Reno, 1664 N. Virginia Street, Reno, NV 89557, USA
E-mail: jepark@unr.edu
[b] V. Faramarzi[+]
Department of BioNano Technology, Gachon University, 1342 Seongnam-Daero, Sujeong-Gu, Seongnam-si 13120, Republic of Korea
[c] G. Jabbour, J. Park
School of Electrical Engineering and Computer Science, University of Ottawa, Ottawa, ON K1 N 6 N5, Canada
[+] These authors contributed equally.

at the conductor-dielectric interface. Due to a significant mismatch between the wavevector of surface plasmons and incident light coupling between surface plasmons, free-space electromagnetic waves still need to be improved, preventing the realization of plasmonic devices. However, the SPR detection technique typically requires optical coupling configurations, including prism couplers,[36] grating couplers,[37] and waveguide couplers[38] to excite surface plasmons. The need for bulky optical components in the SPR technique hinders system miniaturization and integration with other platforms, such as microfluidic devices.[39] Therefore, device integration in nanophotonics becomes challenging. Recent advances in nanotechnology have inspired the development of miniaturized nanophotonic systems that support strong light-matter interactions and drastically confine light in small volumes, enabling ultralow detection limits and ultimate on-chip integration.[40] The limitations of conventional SPR sensors led to emerging PCFs as a promising candidate for SPR-based biosensing due to their unique optical properties such as high optical confinement, controllable birefringence, possibility to control light propagation, single mode propagation, confinement loss, and design flexibility.[41–43]

2. Fiber-Optic-Based Biosensors

In recent years, biological recognition elements have revolutionized analytical chemistry, which is crucial in advancing

Sareh Vatani received her B.S. degree in Electrical Engineering from Bu-Ali Sina University, Hamedan, Iran, in 2016, and her M.S. degree in Electrical Engineering (Micro/Nano Electronic Devices) from Tarbiat Modares University, Tehran, Iran, in 2020. She is pursuing a Ph.D. in Electrical Engineering at the University of Nevada, Reno. From 2020 to 2022, she was a Research Assistant at Tarbiat Modares University. Her research interests include the development of surface plasmon resonance, designing biophotonic devices using SPR, and fabricating MEMS and NEMS devices.

Jeshurun Biney (Student Member, IEEE) is a biomedical engineering graduate student in the Electrical and Biomedical Engineering department at the University of Nevada, Reno (UNR). He completed his undergraduate studies in 2017 at the Ulsan National Institute of Science and Technology, South Korea, double majoring in Chemical Engineering and Bioengineering. Jeshurun's research focuses on biosensors for detection and diagnosis. He has worked with renowned researchers in medical instrumentation and microfluidics. He participated in an Undergraduate Research Opportunity Program in 2015 and 2016 with Dr. Marc Madou at UC Irvine and Dr. Suichi Takayama at the University of Michigan, Ann Arbor.

Vahid Faramarzi is a Postdoctoral Fellow in the Electrical Engineering department at Gachon University, South Korea. He holds a PhD in Electrical Engineering from Tarbiat Modares University, Tehran, Iran. From 2018 to 2020, he was a Visiting Scholar at Holonyak Micro and Nanotechnology Laboratory, University of Illinois Urbana-Champaign, working with Prof. Rashid Bashir on point-of-care diagnostic and analysis platforms. He also researched at the Carle Cancer Institute-Biomedical Research Center (2018-2019). His research interests include 2D materials-based electrical biosensors, DNA sequencing with nanopore technology, flexible and stretchable bioelectronics, and nanophotonic devices for single molecule detection.

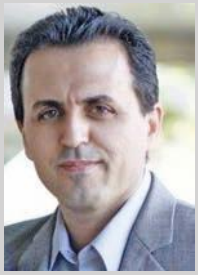

Ghassan Jabbour, PhD is a Canada Research Chair Tier 1 in Engineered Advanced Materials and Devices and Professor of the School of Electrical Engineering and Computer Science at the University of Ottawa. He has dedicated more than 18 years to serving as the Director and Founding Director of major research centers specializing in printed and flexible photonic and electronic devices. He has numerous awards, including the Best Poster Award (2) from the National Academy of Engineering/Engineering Academy of Japan/Japan Science and Technology Agency 2006 Japan-America Frontiers of Engineering Symposium; Distinguished Professor of Finland Award from the Academy of Finland, and the Hariri Foundation Excellence Award, to mention a few. He is an SPIE Fellow and an EOS Fellow for his achievements in flexible and printed photonics and electronics.

Jeongwon Park, PhD (Senior Member, IEEE), is an Associate Professor in the Department of Electrical and Biomedical Engineering at the University of Nevada, Reno, since July 2019. He was an Associate Professor at the University of Ottawa from 2016 to 2021 and a Scientist at SLAC National Accelerator Laboratory, Stanford, from 2014 to 2016. He is currently an Adjunct Professor at the University of Ottawa. Previously, he was a Senior Technologist at Applied Materials (2008–2014), a Guest Researcher at Lawrence Berkeley National Laboratories (2005–2008), an Adjunct Professor at Santa Clara University (2009–2016), and a Visiting Scholar at Stanford (2013–2014).

highly sensitive and selective chemical analyses. Central to this revolution are optical fiber-based biosensors, which have become essential in exploring these elements. Characterized by their exceptional sensitivity, specificity, and adaptability, these biosensors perfectly embody the IUPAC's definition by seamlessly integrating biological recognition components with transducers to yield quantitative or semi-quantitative data. This discussion aims to unpack the recent technological progress, diverse applications, and the prospective trajectory of optical fiber-based biosensors in analytical chemistry.[44,45] Biosensors are distinguished by their specificity and sensitivity, crucially depending on the unique binding properties of bioreceptors and the transduction efficiency. Fiber optic biosensors have become increasingly prominent due to their remarkable stability,[46] cost-effectiveness,[47] and innovative capacity for broad-spectrum detection of biological analytes.[48]

Due to their sensitivity and specificity, fiber-optic biosensors are becoming a pivotal technology in medical diagnostics. Generally, these biosensors can be categorized into wavelength[49] and intensity-based[50] systems. Wavelength-based biosensors utilize light wavelength variations as the sensing mechanism and include subcategories such as gratings, interferometers, and resonances. Within these, SPR, Localized Surface Plasmon Resonance (LSPR), and Fiber Bragg Gratings (FBG) are notable technologies that have been the focus of recent advancements and applications in medical diagnostics.[51,52] Surface Plasmon Resonance (SPR) sensors detect surface changes using surface plasmons at metal-dielectric interfaces, offering high sensitivity but requiring precise wavelength control. Tilted Fiber Bragg Gratings (TFBGs) enhance sensitivity through selective wavelength response but are sensitive to temperature changes. Long Period Fiber Gratings (LPFGs) provide high refractive index sensitivity yet can be influenced by temperature.

Interferometers, such as all-fiber and Fabry-Pérot types, offer high sensitivity but are complex to design and calibrate. Resonance-based sensors like LSPR and LMR provide specialized detection capabilities; LSPR excels in biomedical applications through localized electromagnetic fields around metallic nanoparticles. LMR sensors detect temperature and refractive index changes through thin films or waveguides. On the other hand, intensity-based biosensors detect changes in light intensity, subdivided into luminescence and absorption. Luminescence-based sensors are further divided into those that enhance or quench the signal. In contrast, absorption-based sensors use evanescent wave phenomena and resonant phenomena to detect the presence of analytes.[46,48] Absorption sensors use evanescent waves for real-time, label-free detection but may lack sensitivity compared to other methods. Resonance-based absorption sensors are highly selective but challenging to calibrate. Each subcategory is tailored to specific types of analytes and applications, ranging from detecting small molecules to monitoring complex biochemical interactions. The development of these sensors continues to advance, focusing on increasing their sensitivity, specificity, and ease of integration into existing medical technologies.[53,54] These different biosensors offer diverse mechanisms and applications, and their continued development hinges on advancements in optical engineering and material science. Figure 1 shows the basic structure of a biosensor.

These biosensors incorporate a variety of fiber geometries, including side-polished,[55] D-shaped[56] U-shaped[57] and tapered fibers,[58] as well as PCF[53] and grating fibers, all designed to maximize environmental interaction.[59] Mechanisms like SPR and LSPR are critical to their functionality, enabling sensitive detection of a wide range of analytes.[52] This discussion explores the cutting-edge technological developments, diverse applications, and prospective advancements of fiber optic biosensors.

Optical fiber biosensors have become indispensable tools across various sectors, such as medical diagnostics, environmental monitoring, and food safety, primarily due to their efficiency in detecting biomarkers, pathogens, and toxins. Integrating nanomaterials has significantly enhanced their capability to analyze low-concentration analytes, improving sensor performance sensitively. This enhancement is evident in advanced sensor designs incorporating long-period gratings (LPG) and tilted fiber gratings (TFG), which offer increased sensitivity. These biosensors can monitor two crucial parameters: wavelength shifts and intensity variations.[60,61] Wavelength-based optical fiber biosensors, in particular, have undergone significant scrutiny and development over the past decade. Studies have revealed three primary approaches to designing these biosensors, underscoring the advantages of utilizing wavelength-shift measurements. In the context of intensity-based optical fiber biosensors, recent advancements bring an expanded perspective on these technologies' developmental progress and potential applications.[50] By exploring the latest innovations in this field, one gains a comprehensive understanding of the state and scope of optical fiber biosensors as versatile and powerful platforms for diverse applications.

Fiber-optic biosensors have significant applications in both in vivo and in vitro environments, offering precise sensing and monitoring capabilities crucial for biomedical research and healthcare. In vivo applications directly use biosensors within living organisms to monitor physiological parameters in real-time. Huang et al.[62] utilized SiO_2-coated PVA (polyvinyl alcohol) hydrogel fibers as neural probes, which can be implanted into the brain to monitor neural activity with minimal tissue damage. Their SiO_2 coating enhances signal transduction and ensures stability in the harsh neural environment, enabling accurate monitoring of brain activity over extended periods. Another crucial in vivo application is the monitoring of glucose levels in mice.[63] Fiber-optic biosensors can continuously monitor blood glucose levels, providing valuable data for diabetes research and treatment. The ability to track glucose

Figure 1. Biosensor Structure. Created with BioRender.com.

levels in real-time with minimal invasiveness is essential for understanding glucose metabolism and the effects of diabetes treatments. In vitro applications analyze biological samples outside living organisms in controlled environments, such as labs or diagnostic centers. This technology is illustrated by applying the gold nanorod's localized surface plasmon resonance (LSPR) for detecting C-reactive protein- a well-known biomarker for inflammatory disorders.[64] According to the study, these gold nanorods are highly sensitive and specific in detecting a range of biomolecules, attributes attributable to their distinctive optical properties. The gold nanorods exhibit localized surface plasmon resonance (LSPR), which enhances their interaction with target molecules, making them suitable for detecting low concentrations of analytes in complex biological samples.[65,66] The use of fiber-optic biosensors for cancer cell detection by Loyez et al.[67] is another instance of an in vitro application. These sensors can identify cancer-specific biomarkers in body fluids or tissue samples, providing early diagnosis and monitoring of cancer progression. The high sensitivity and specificity of these sensors enable the detection of even small numbers of cancer cells, which is crucial for timely intervention. Fiber-optic biosensors offer significant advancements in both in vivo and in vitro sensing and monitoring. Their ability to provide real-time, sensitive, and specific detection of various biological substances makes them invaluable tools in biomedical research and clinical diagnostics.

A recent exploration into the utility of fiber optic-based biosensors for precise medical applications was conducted by Luo et al. This study emphasizes the incorporation of fiber optics into biosensing to account for individual variability in clinical diagnostics, thereby advancing the field of precision medicine.[68] Another innovative approach by Zhang et al. utilized a U-fiber-based biosensor, demonstrating a temperature-compensated technique for measuring acetylcholine, which has potential applications in neurological disorder diagnostics.[46] Additionally, Rashidova et al. developed a functionalized optical fiber ball-shaped biosensor for the label-free detection of salivary IL-8 protein, showcasing a promising tool for non-invasive medical diagnostics.[48]

Recent studies in the emerging field of fiber optic-based biosensors have paved the way for innovative diagnostic tools. Luo et al. advanced precision medicine with new structural fiber optics designs that enhance biocompatibility and label-free detection.[68] Zhang et al. contributed a U-fiber biosensor with a temperature-compensated mechanism for acetylcholine measurement, indicating a leap forward in neurological diagnostics.[69] Murugan et al.'s plasmonic fiber-optic biosensor demonstrated one-step detection of SARS-CoV-2, signaling a breakthrough in pandemic response tools.[70] The table below provides a concise summary of various research findings, illustrating the versatility and depth of this technology across different medical applications.

Ran et al.[71] contributed significantly to the field of optical biosensing by introducing a temperature compensation method using microfiber Bragg gating. This novel approach addresses the challenges posed by temperature fluctuations on the accuracy of fiber optic-based biosensors. The technique involves measuring temperature and RI changes, enhancing the detection reliability of the cardiac biomarker cTn-1. This method improves the immunoreaction dynamics and reduces variability between individual samples, a crucial advancement in the consistency and reliability of biosensing technologies.

Research conducted on silica-functionalized carbon dots synthesized from curcumin and DMF, as described in a study by Sangubotla,[72] shows promising results in biosensing. The immobilization of these dots with laccase enzyme on optical fibers exhibits high sensitivity for dopamine detection and potential in multi-color imaging applications, marking a significant stride in optical biosensing technology. Silica-functionalized carbon dots were prepared using APTES and immobilized with laccase enzyme (bioprobe). The bioprobe was immobilized on the optical fiber using ethyl cellulose by a facile dip-coating method. Bioprobe showed high PL sensitivity for dopamine with low DOL of 41.2 and 46.4 nM. Bioprobe was investigated for multi-color imaging applications in human neuroblastoma cells (SH-SY5Y) and optical fiber.

Esposito et al.[73] designed a label-free fiber optic biosensor for vitamin D detection in an innovative development. Utilizing a GO layer on a long-period grating in a double cladding fiber, this biosensor can detect 25-hydroxyvitamin D3 concentrations with exceptional sensitivity, detecting 25-hydroxyvitamin D3 (25(OH)D3) concentrations within 1–1000 ng/mL, and a low limit of detection (LOD) below 1 ng/mL. The device's ability to measure vitamin D levels non-invasively presents new healthcare monitoring and diagnostics opportunities.

Pasquardini and colleagues[74] developed an SPR plastic optical fiber biosensor metalized with a 60 nm layer of gold and interrogated with white light. The sensor was made specific by coupling it with an anti-amylase antibody to detect pancreatic amylase in drain effluent. The POF-biosensor showed selectivity for amylase, a calibration curve log-linear in the range of 0.8–25.8 U/L, and a LOD of ~0.5 U/L. This biosensor, characterized by its specificity and optimized surface derivatization, demonstrates excellent potential for rapid and accurate bedside assessments in clinical settings.

Li et al.[75] explored a novel method for glucose detection using a localized LSPR sensor with a serial quadruple tapered structure. Enhanced with gold nanoparticles (AuNPs) and carbon-based nanomaterials, this sensor shows exceptional sensitivity and selectivity for glucose. (AuNPs) are immobilized on the serial quadruple taper fiber (SQTF) to induce LSPR. To achieve high selectivity for glucose, the surface of the SQTF probe is functionalized with glucose oxidase (GOx) enzyme. This strategic functionalization results in enhanced sensitivity and selectivity of the sensor for glucose detection. The sensitivity and LOD of the functionalized probe structure are 1.04 nm/mM and 0.24 mM over a linear range of 0 mM–10 mM, respectively. The SQTF probe, functionalized with glucose oxidase enzyme, demonstrates potential in medical diagnostics, particularly in monitoring and managing glucose-related health conditions.

Lobry et al. (2020) conducted a recent study focusing on developing a highly sensitive biosensor for detecting Human Epidermal Growth Factor Receptor-2 (HER2), a key biomarker in

breast cancer was carried out by Lobry et al.[76] This advanced biosensor utilizes plasmonic tilted fiber Bragg gratings (TFBGs), known for their precision and sensitivity in biochemical detection. The uniqueness of this biosensor lies in its triple-strategy approach, enhancing both performance and robustness. The sensor's substrate is made from a single polarization fiber (SPF), while its demodulation technique involves tracking an unusual feature in the lower envelope of the cladding mode resonances spectrum. This method significantly increases the sensor's sensitivity, yielding wavelength shifts much more significant than those observed in traditional approaches based on individual mode tracking.

Moreover, the sensor's response is amplified through a sandwich assay using specific antibodies, further enhancing its detection capabilities. The development of this aptasensor marks a significant stride in point-of-care biomedical measurements, offering a practical and convenient tool for the early detection of breast cancer. The ability of this biosensor to accurately detect the HER2 protein opens up new possibilities in cancer diagnostics, potentially leading to earlier and more effective treatment strategies for patients.

Fiber-optic biosensors have evolved into sophisticated devices critical for various applications. Advancements have led to their classification primarily into two broad types based on their operation principles: wavelength-based and intensity-based sensors. Wavelength-based sensors include gratings, interferometers, and resonances, each offering unique environmental and biological sensing capabilities. Figure 2 depicts the condensed classification.

Table 1 summarizes the extensive research in optical biosensors, including details on target analytes, DOL, and principles. Despite their advantages, fiber-optic biosensors face challenges like light source instability, environmental influences like temperature and humidity, and miniaturization issues.[46,77,78] Future developments are expected to overcome these challenges, enhance micro-structural stability, improve immobilization protocols, and expand clinical, environmental, and industrial applications.[79,80] The evolution of these biosensors is likely to see more integration with nanotechnology, offering more compact, efficient, and versatile sensing solutions. Fiber optic biosensors represent a significant advancement in biosensor technology, offering a range of applications and potential for further development. Their miniaturization ability, combined with advancements in optical technology and nanomaterials, positions them as crucial instruments in various scientific and practical fields.

3. Plasmonic Materials

3.1. Graphene

Graphene, characterized by its hexagonal lattice structure formed by atomically thin carbon sheets,[92] emerges as a distinct plasmonic material adept at functioning across the mid-infrared (IR) to terahertz (THz) regions of the spectrum. A noteworthy feature is the adjustability of graphene's optical constants, including permittivity and refractive index, achievable through applying a gate voltage—a capability surpassing traditional metal-based plasmonic materials.[93,94] While conventional plasmonic materials such as Au, Ag, and Al are effective in inducing surface plasmon polaritons (SPPs) at wavelengths below the mid-IR region, their utility diminishes at longer wavelengths. This limitation primarily arises from their inherent material properties, where significant optical losses occur due to inter-band transitions and electron scattering. In particular, at mid-IR to terahertz (THz) frequencies, these materials exhibit pronounced damping of plasmonic modes, which severely restricts their performance in plasmonic and metamaterial devices aimed at these frequencies.[95] Such drawbacks underscore the necessity for alternative materials that can support efficient plasmonic activity in the mid-IR and THz domains without the substantial loss mechanisms that hamper conventional metals.[96] While conventional plasmonic materials like Au, Ag, and Al induce surface plasmon polaritons (SPPs) at wavelengths beneath the mid-IR region, a growing demand exists for SPPs, specifically in the mid-IR and THz domains.[95] Graphene's outstanding electrical, optical, and chemical properties, stemming from its unique Dirac cone-type bandgap structure, encompass high carrier mobility, rapid photo response, and comprehensive photodetection spanning from ultraviolet to THz. These attributes, coupled with flexibility and cost-effective-

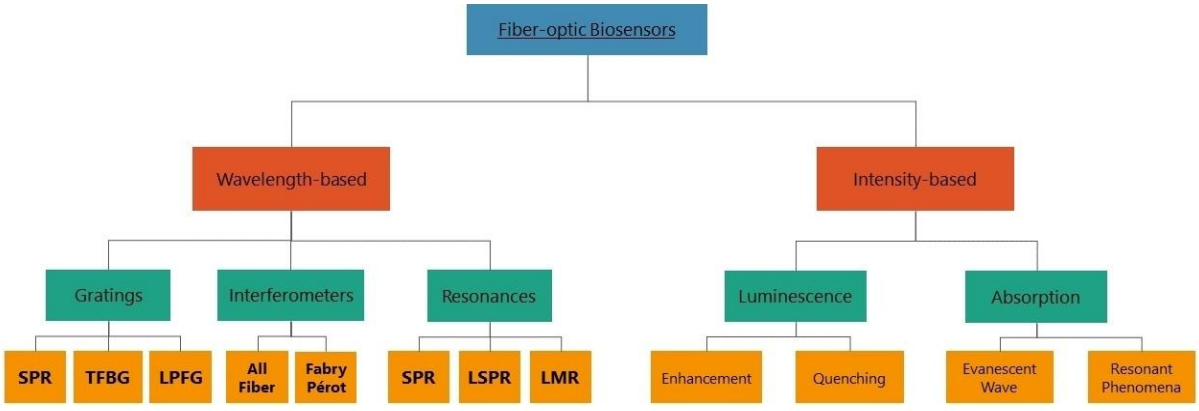

Figure 2. Classification of fiber-optic biosensors.

Table 1. Summary of Recent Advances in Optical Fiber Biosensor Technologies.

Target Analyte	LOD (low detection limit)	Approved cut-off levels for commercialization[a]	Taper Geometry	Detection Principle	References	Year
Cardiac Troponin I–cTn-1	13.5 ng/mL	$>$0.10 ng/mL	N/A	Single Microfiber Bragg Grating	[71]	2021
Vitamin D	1 ng/mL	4~10 ng/mL	N/A	Long Period Grating (LPG)	[73]	2021
Cardiac Troponin I–cTn-1	96.26 ng/mL	$>$0.10 ng/mL	N/A	Localized Surface Plasmon Resonance (LSPR)	[81]	2022
BSA	971 ng/mL	$<$250 ng/mL	N/A	Surface Plasmon Polaritons (SPPs)	[82]	2020
MicroRNA	1.33×10^{-5} ng/μL	0.05~100 ng/μL	U-shaped	Surface Plasmon Resonance (SPR)	[83]	2020
Dopamine	46.4 nM	N/A	N/A	Fluorescence Plastic Cladded Silica Fiber	[72]	2021
MutS protein	0.49 nM	N/A	N/A	Plasmon Resonance (FOPPR)	[84]	2021
Human IgG	0.8 nM	NA	N/A	Localized Surface Plasmon Resonance (LSPR)	[85]	2020
Glucose	4.32 mg/dL	30~396 mg/dL	N/A	Localized Surface Plasmon Resonance (LSPR)	[75]	2022
SARS-CoV-2	10^{-9} nM	$\leq5.0\times10^{2}$ pfu/ml	U-bent	Portable Plasmonic Fiber-Optic Absorbance Biosensor (P-FAB)	[70]	2020
tDNA	1 pM	N/A	N/A	Surface Plasmon Resonance (SPR)	[86]	2022
Staphylococcus aureus	1×10^{4} CFU/mL	N/A	N/A	Quantum Dots Immunofluorescence	[87]	2021
Pathogenic E. coli	10 CFU/mL	depends on strain	N/A	Mach-Zehnder Interferometer (μIMZI)	[88]	2021
Pancreatic Amylase	0.5 U/L	2×10^{-4}~2×10^{-1} U/L	N/A	Surface Plasmon Resonance (SPR)	[74]	2021
MDA-MB-415 and HEK293 (CTCs)	49 cells/mL	N/A	N/A	Surface Plasmon Resonance (SPR)	[67]	2020
Human IgG	N/A	N/A	D-type	Surface Plasmon Resonance (SPR)	[89]	2020
HER2	N/A	N/A	N/A	Surface Plasmon Resonance (SPR)	[76]	2020
Cancer Cells (MDA-MB-231, MCF-7, Jurkat and PC12)	N/A	N/A	Crescent shape	Surface Plasmon Resonance (SPR)	[90]	2021
blood cancer cells	N/A	N/A	hexagonal-shaped	Twin-Core Photonic Crystal Fiber (TC-PCF)	[91]	2020

[a] Cut-off levels for commercialization were obtained by averaging the values of existing devices that have FDA approval as of May 2024.

ness, position graphene as a promising material offering advantages unattainable through conventional bulk technologies.[97] The integration of graphene into various biosensor structures has significantly advanced biosensing capabilities. One prominent design is the Graphene Field-Effect Transistor (GFET),[98] utilizing graphene's exceptional electrical properties to detect biomolecular interactions through conductivity changes. Another approach involves Graphene Oxide (GO) nanosheets,[99] which offer a high surface area for diverse biosensing applications, such as fluorescence, electrochemical, or impedance-based detection. Electrochemical biosensors benefit from graphene's conductivity, forming a platform for highly sensitive detection of biomolecules.[100] Graphene Quantum Dots (GQDs)[101] contribute to biosensing through unique electronic and optical properties, enhancing detection sensitivity. Additionally, graphene-based nanocomposites[102] exhibit improved biosensing performance by combining graphene with other nanomaterials. Integration into the structure of optical fibers[103] and PCFs[104] allows for optical biosensing applications, demonstrated in Figure 3(a) and (c), respectively. Furthermore, graphene stands out as an excellent material for molecular adsorption owing to its expansive surface area and abundant π configuration. Serving as a biomolecular recognition element (BRE), it provides a prominent platform for the adsorption of diverse biomolecules. This, in turn, leads to a modification in the propagation constant of Surface Plasmon Polariton (SPP) modes, inducing a substantial RI variation on the graphene-silver interface.[105] In 2010, a paper reported by Wu et al.,[106] In comparison to the conventional gold thin film SPR biosensor, introducing a few layers of graphene enhances sensitivity by $(1+0.025\ \mathrm{L})\times\gamma$ times (where $\gamma>1$). This heightened sensitivity stems from graphene's ability to strongly and

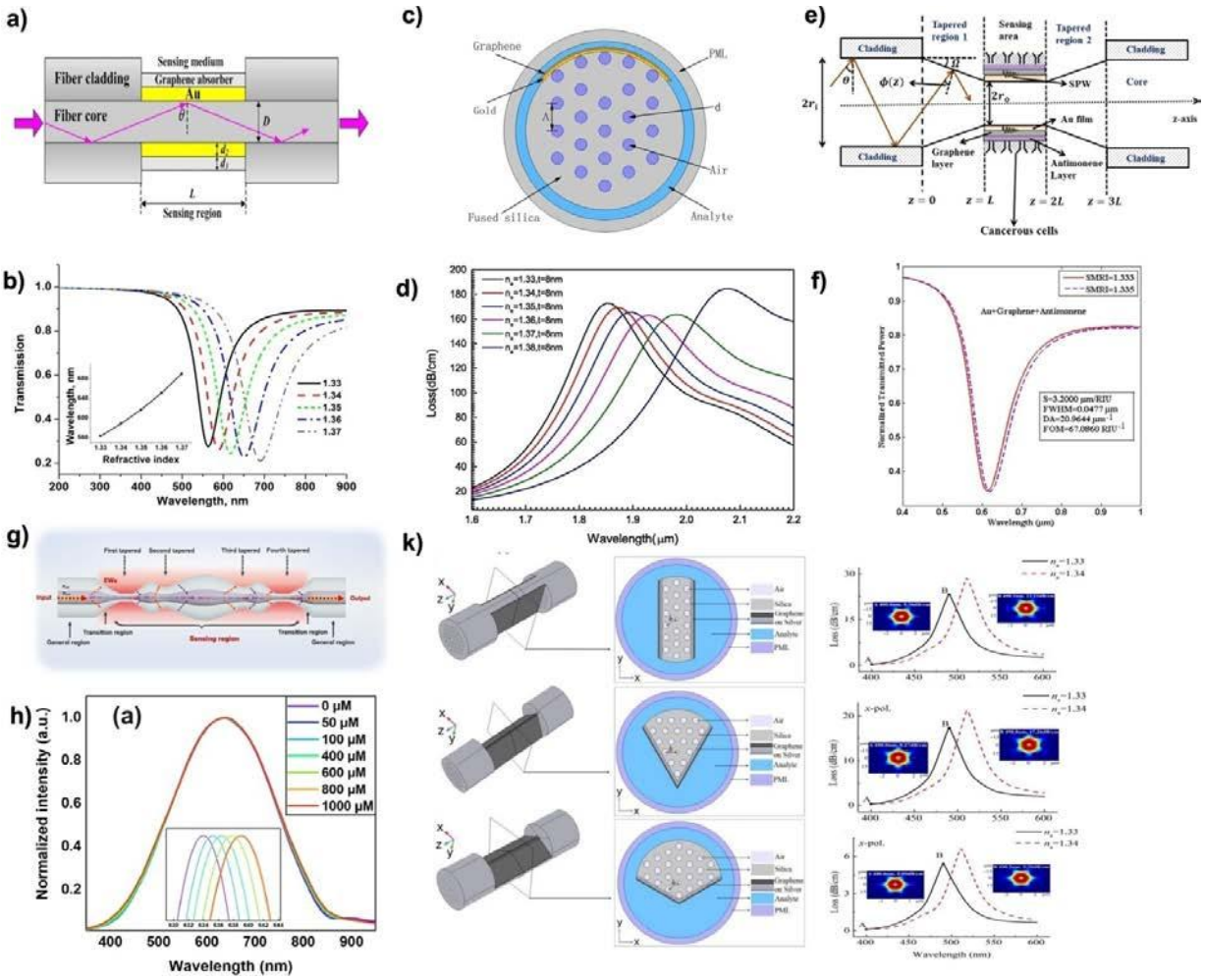

Figure 3. a) Illustrated schematic of the proposed SPR fiber biosensor incorporating a graphene sensing layer. b) Transmission spectra of the proposed SPR fiber biosensor as the surrounding refractive index (SRI) varies. Inset: the correlation between resonance wavelength and SRI[103] (Reproduced with permission from Ref[103] Copyright 2015 IEEE). c) Diagram depicting the designed sensor. d) Spectral loss variations of the designed sensor as the RI (n_a) ranges from 1.33 to 1.38 in increments of 0.01[104] (Reproduced with permission from Ref,[104] Copyright 2019 ScienceDirect). e) Schematic representation of the proposed tapered fiber optic SPR biosensor. f) Illustrates the transmitted SPR spectra of the proposed fiber sensing setup (Au + graphene + antimonene) at TR 1.0, indicating the untapered core[108] (CreativeCommonsLicense4.0., with permission from 2023 ACS Publication). g) Schematic of humanoid tapered optical fiber (HTOF) based sensor probe. h) The LSPR spectra were recorded for each concentration, ranging from low to high[109] (CreativeCommonsLicense4.0., with permission from Optica Publication). k) The diagrams depict the 3D and cross-sectional views of SPR sensors, utilizing double-sided polished MOF coated with graphene-on-silver layers. The angles between the two polishing planes (θ) are illustrated as follows: 0°, 60°, and 120°, from top to bottom, respectively. The spectra on the right side, from top to bottom, represent the loss spectra of the x-polarized core mode of the double-sided polished MOF-SPR sensor with θ = 0°, 60°, and 120°, respectively. The surface plasmon polariton (SPP) modes on the graphene-on-silver layer exhibit polarization in both the x and y directions[110] (CreativeCommonsLicense4.0., with permission from IEEE).

stably adsorb biomolecules with carbon-based ring structures, serving as a biomolecular recognition element and augmenting adsorption efficiency (E) by a factor of γ. Additionally, graphene's optical properties modify SPR curves, boosting sensitivity to Surrounding refractive index change (SRI) by 25% for L = 10. An overall sensitivity increase of 5 times occurs if graphene adsorbs 4 times more biomolecules ($\gamma = 4$).

Recently, the article[107] introduced a highly sensitive D-shaped optical fiber sensor for ethanol concentration detection, employing SPR technology with a gold plasmonic layer and a molecularly imprinted polymer (MIP) layer for enhanced bonding with molecules. A graphene thin layer is incorporated to improve sensor life and performance. The sensor design features a GeO_2 circular core, SiO_2-fused cladding, and a 15 μm total fiber diameter. The MIP layer enhances metal adhesiveness, and an Au film with a 7 nm graphene layer between silica (SiO_2) and gold enhances sensing ability while reducing oxidation. Also, in Saccomandi's paper[108] depicted in Figure 3(e and f), the Au film is enhanced for improved sensitivity and efficiency in the SPR biosensor design by coating monolayers of graphene and antimonene. This modification enhances biomolecule adsorption on the surface, which is beneficial for early-stage cancer detection. In the study undertaken by Zhang in 2023[109] shown in Figure 3(g and h), a novel humanoid-shaped tapered optical fiber (HTOF) structure-based LSPR sensor probe was developed Using a single-mode fiber (SMF) for the detection of histamine. The sensor was functionalized with GO/MWCNTs, effectively increasing the specific surface area of the

fiber probe. This enhancement provided more attachment sites for immobilizing AuNPs and functionalizing the diamine oxidase (DAO) enzyme. The experimental results revealed a linear range of 0–1000 μM, a sensitivity of 5.5 nm/mM, and a LOD of 59.45 μM. Leveraging the LSPR phenomenon, this sensor demonstrates high sensitivity, low LOD, and fast response, making it a promising optical fiber biosensor for histamine detection. In Hou et al. paper,[110] as shown in Figure 3(k), a thin silver layer is applied to the polished surface, covered by multilayer graphene, forming the graphene-on-silver layer for direct analyte contact. With polishing plane angles of 0°, 60°, and 120°, the sensors were evaluated using wavelength and amplitude interrogations. Remarkably, all orientations exhibited a maximum sensitivity of 2070 in x-polarization, showcasing the sensors' consistent and robust performance.

3.2. TMDCs

Transition metal dichalcogenides (TMDC) materials, represented by MX_2, showcase distinctive optical and optoelectronic characteristics. Comprising a hexagonal arrangement of transition metal atoms situated between two hexagonal lattices of chalcogenide atoms, MX_2 materials emerge as promising contenders in the semiconductor industry. Their applications span a wide array, encompassing high-speed electronics, flexible devices, next-generation solar cells, touchscreen display panels, DNA sequencing, and personalized medicine, among other innovative fields.[111] In addition to graphene, two-dimensional materials like TMDCs, exemplified by WS_2,[112] MoS_2,[113] $MoSe_2$,[68] and WSe_2,[114] present compelling opportunities for enhancing biosensor sensitivity. Their elevated surface-to-volume ratio and adaptable biocompatibility contribute to heightened sensitivity.[115]

Moreover, their high dielectric constant enhances the metal's light energy absorption.[116] These materials can also serve as protective layers when coated on metal films, safeguarding against oxidation and extending the biosensors' durability.[117] Utilizing a heterostructure comprised of MoS_2/WS_2 on the Ag metal layer in the optical fiber-based sensor, Jing et al.[118] achieved a notable sensitivity of 3127.18 nm/RIU, accompanied by a figure of merit reaching up to 70.04 RIU^{-1} in their study. Aiming to enhance the sensitivity, Wang et al.[119] designed taper-in-taper structure sensing probes using single-mode fiber. Immobilizing AuNPs, MoS_2-NPs, and CeO_2-NPs on the probe's sensing region enhances the LSPR effect. Li et al. conducted research[120] comparing the sensing system with and without MoS_2, analyzing the spectral response to the surrounding refractive index. Results showed that the optical fiber SPR sensor with MoS_2 exhibited approximately 24% higher bulk RI sensitivity than the sensor with pure metal films. Specifically, the sensitivity of the optical fiber SPR sensor with pure metal film (Ag) was about 2888 nm/RIU. However, with the addition of MoS_2, the resonance wavelength shifted from 628 nm to 773 nm under the same conditions, resulting in a sensitivity of 3596 nm/RIU. Also, In the study conducted by Odac and Aydemir (2021),[121] the 2D TMDC materials cover the Au/Ag bimetallic layer. For a slight change in the RI 0.0025 of the sensing medium, the monolayer $MoSe_2$ exhibits the highest sensitivity of 8096 nm/RIU.

Conversely, the monolayer WS_2 demonstrates the highest accuracy, 0.34, and the figure of merit is 136.89 RIU^{-1} values. Interestingly, while the sensitivity of the MoS_2 structure increases with the number of layers, other TMDC materials do not follow the same trend. Ouyang et al.[122] reported that a notably low minimum reflectivity of 3.2560×10^{-8} was achieved at an excitation wavelength of 1024 nm, indicating nearly complete light energy transfer (≈100%) into plasmon resonance energy. This near-zero reflectivity at the resonance dip results in an unprecedented plasmonic sensitivity with adding $MoSe_2$ of 1.1×10^{7} deg/RIU, surpassing by three orders of magnitude the sensitivities observed in commercial plasmonic sensors utilizing bare metallic sensing substrates. Platinum diselenide ($PtSe_2$), as a novel 2D transition metal dichalcogenide, demonstrates a thickness-dependent refractive index, leading to captivating optical characteristics. Guo et al. reported[123] that the sensor achieves an impressive detection limit for RI changes, reduced to 5×10^{-7} RIU, representing a substantial 2 orders of magnitude improvement compared to conventional gold sensors. This advancement corresponds to a remarkable 1000-fold enhancement in sensitivity for biomolecule detection. The sensor described in the study by X. Zhao et al.[124] employs various 2D TMDCs coated on both surfaces of a metal film. Through optimization of structural parameters, the angular sensitivity can reach up to 315.5 deg/RIU with a combination of 7 layers of WS_2 and a 36 nm Al thin film. This represents a significant improvement, achieving 3.3 times the sensitivity compared to conventional structures based solely on a single Al thin film. The utilization of different TMDC materials on both sides of the metal layer emerges as the primary reason behind this enhanced sensitivity.

3.3. Germanium

MX series compounds are considered promising materials for optoelectronic and electronic devices due to their remarkable mechanical flexibility, high light absorption, thermoelectric coefficient, carrier mobility, abundance, low toxicity, and stability.[125,126] Li et al. demonstrated that the GeS monolayer possesses significantly higher carrier mobility (3680 cm^2V^{-1}) than MoS_2 monolayers.[127] Sensor studies indicate the highest sensitivities for GeS–Al, GeS–Ag, and GeS–Au films at 320 deg/RIU, 295 deg/RIU, and 260 deg/RIU, respectively, surpassing conventional SPR sensors based on Al/Ag/Au films at 111 deg/RIU, 117 deg/RIU, and 139 deg/RIU, respectively.[128] A study executed by Zhao[34] illustrates a substantial advancement in sensitivity for RI detection, achieving an optimized sensitivity of 3581.2 nm/RIU and a figure of merit of 14.37 RIU^{-1}. This improvement, nearly 80% greater than conventional SPR sensors, results from covering the gold film with stable and cost-effective Germanium selenide (GeSe) nanosheets. GeSe nanosheets, strategically placed at the sensing interface with analytes, expedite detecting RI changes, enhancing the sensor's

responsiveness and efficiency. The proposed SPR sensor is based on a $Ge_2Sb_2Te_5$-modified gold film (Au-GST),[129] characterized by stability and non-volatility. The GST is known for its ability to transform between crystalline and amorphous states, making it a key material in optical storage applications. Its exceptional performance has prompted exploration in the sensing field. The combination of GST with SPR sensors is considered to enhance sensitivity. GST's high dielectric constant can shift SPR sensing bands to the near-infrared range. A cascaded dual-channel SPR fiber sensor is demonstrated, with GST coating applied to the Au film to red-shift sensing bands. Channel I is configured with an Au-coated optical fiber surface, exhibiting sensing bands from 596 nm to 793 nm. Channel II features an Au-GST composite film, showcasing bands from 1045 nm to 1421 nm. With an RI measuring range of 1.333–1.403, average sensitivities of 2781 nm/RIU and 5226 nm/RIU are achieved, respectively. In their study, Liu et al.[130] conducted tests using 25 nm of $Ge_2Sb_2Te_5$ on 50 nm of Au deposited on unclad multimode fiber, yielding a sensitivity of 5210 nm/RIU. Zhao et al.[131] introduce an SPR sensor utilizing a D-shaped germanium-doped PCF shown in Figure 4(a), analyzed using the finite element method (FEM) to assess structural parameters and germanium-doped concentration, lattice pitch, and air hole size. The effect of germanium concentration on birefringence is examined, with an optimal wavelength sensitivity of 5600 nm/RIU observed at an RI of 1.37. The sensor demonstrates a maximum birefringence of 1.06×10^{-2} and a resolution of 1.78×10^{-5} RIU with high linearity. The study by Cunha et al.[132] presents a novel plasmonic sensor model employing a microstructured optical fiber for RI detection, incorporating GeO_2 dopings within a circular defect. While increasing the dopant concentration slightly reduces sensitivity, the sensor's adaptable design and extended detection range offer promising applications for diverse analyte detection in practical sensing environments. Gangwar et al.[133] demonstrated in Figure 4(b) a D-shaped optical fiber SPR sensor where a gold film is positioned at the flat portion of the fiber and GeO_2 is doped into the silica core. Through FEM analysis, sensing properties are explored, achieving a maximum sensitivity of 20863.20 nm/RIU, resolution of 4.79×10^{-6} RIU, and figure of merit of 308.38 RIU^{-1} for an RI of 1.43.

3.4. Black Phosphorous

Black phosphorus (BP), a novel 2D semiconducting material, stands out for its high carrier mobility and tunable direct bandgap, making it highly promising for photonic and optoelectronic device applications. First, in contrast to other 2D materials, the layered BP possesses higher molecular adsorption energy and a larger surface-to-volume ratio, which can maximize the adsorption effect of chemicals.[134,135] Furthermore, its unique puckered structure gives rise to intrinsic anisotropy, which is beneficial in designing new devices. Recent studies have demonstrated the efficiency of BP in various optical sensor applications, such as high-performance humidity sensing, due to its unique electrical, mechanical, and surface properties demonstrated by Yu et al.[136] Figure 5 below shows their experimental setup for sensing humidity. The experiments show that when BP nanosheets are coated, they can effectively adjust transmitted light in the etched single-mode fibers (ESMF) as humidity levels change between 35% and 80%, allowing for rapid humidity sensing in just 7 ms. This research introduces a BP-based optical sensing system that not only performs well in humidity sensing but also presents new possibilities for detecting various vapors and gases in fields like biomedicine and chemistry.[136]

Researchers, including Vasimalla et al.,[137] have developed a high-performance SPR sensor using a hybrid structure of BP and tungsten disulfide (BP-WS_2) to detect DNA hybridization. This sensor design comprises five distinct layers: a fiber core, a layer of silver (Ag), BP, WS_2, and a sensing medium. The choice of materials, particularly the Ag-BP combination and the remarkable properties of WS_2, is central to the sensor's functionality. The BP-WS_2 monolayer, strategically positioned between the Ag metal film and the sensing medium, is critical in enhancing the sensor's sensitivity. This multilayered fiber-optic-based SPR sensor showcases improved sensitivity and heightened detection accuracy in identifying DNA hybridization and single nucleotide polymorphisms (SNPs). This groundbreaking study emphasizes the sensor's superior performance in terms of sensitivity, depth-of-figure-of-merit, and quality factor. These enhanced performance parameters signify a substantial improvement over existing technologies in DNA hybridization sensing.

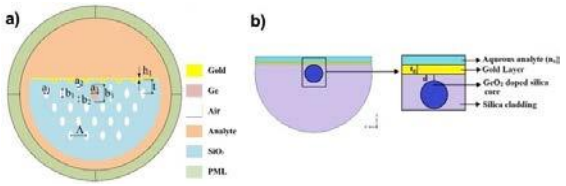

Figure 4. a) The D-shaped PCF sensor model proposed simulated by FEM[131] (CreativeCommonsLicense4.0., with permission from MPDA). b) The fiber is a conventional single-mode fiber. The fiber core, with an RI, denoted as n_{co}, comprises GeO_2 doped silica, facilitating light propagation within the core. The cladding, on the other hand, is made of fused silica[133] (CreativeCommonsLicense4.0., with permission from Springer).

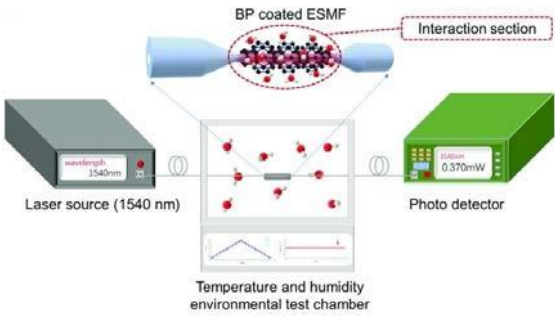

Figure 5. An all-fiber BP-based humidity sensor is created by integrating BP nanosheets with ESMF[136] (Reproduced with permission from Ref[136] Copyright 2020 Wiley).

Zhou et al.[138] have made a remarkable contribution to cancer diagnostics by developing the first black phosphorus (BP)-fiber optic biosensor. This groundbreaking biosensor focuses on the ultra-sensitive detection of Neuron-specific enolase (NSE), a particular biomarker found in various cancers, including neuroendocrine tumors, lung cancer, medullary thyroid cancer, carcinoid tumors, pancreatic endocrine tumors, and melanoma. Implementing the BP-Tilted Fiber Grating (BP-TFG) in this biosensor has demonstrated exceptional sensitivity for detecting NSE biomarkers. With a LOD as low as 1.0 pg/mL, the biosensor's sensitivity surpasses conventional standards by four orders of magnitude lower than the NSE cut-off value for small cell lung cancer (SCLC). This sensitivity is about 100 times greater than biosensors based on GO or AuNPs. The introduction of the BP-fiber optic biosensor represents a significant leap forward in cancer biomarker detection. Its ultra-high sensitivity and specificity are pivotal in enabling the early diagnosis of various cancers and diseases. This advancement enhances the accuracy of cancer detection and opens new horizons in the timely and effective treatment of cancer patients.

Responding to the growing health concerns over bisphenol A (BPA), Qiao's[139] team has successfully integrated BP with hollow-core anti-resonant fiber (HARF) to create a sensor with significantly enhanced BPA detection capabilities. The superior physical attributes of two-dimensional black phosphorus (2D BP) make it an exemplary candidate for constructing the BP-HARF (black phosphorus-hollow-core anti-resonant fiber) complex. This complex offers several distinct benefits: firstly, the inherent flexibility and high adsorption capacity of BP ensures a robust and secure adhesion to the inner surfaces of the HARF; secondly, the atomic-scale thickness of BP maintains the fundamental structure and key optical functionalities of the HARF; and thirdly, the unique characteristics of BP impart functionalities to the complex that are unattainable with traditional materials. This advanced system facilitates a label-free, swift, and economically viable approach for detecting bisphenol A (BPA) in biological fluids and environmental samples.

As a sensitive material, BP has electrostatic adsorption characteristics for lead ions (Pb^{2+}).[140] Capitalizing on this feature, a highly sensitive sensor for detecting trace amounts of lead ions (Pb^{2+}) has been developed by Teng et al.[141] Utilizing light deposition technology, BP nanosheets synthesized via hydrothermal reaction and ultrasound peeling were applied to tapered fibers. The electrostatic interaction between BP and Pb2+ ions leads to shifts in the interference spectrum, enabling the detection of Pb^{2+} concentrations as low as 0.0206 ppb. The LOD of the sensor is 0.0206ppb. Based on BP-integrated tapered fiber, this sensor exhibits rapid response and a very low detection limit, proving its potential for water quality monitoring.

3.5. Silicon

Silicon plays a crucial role in optical fibers- cylindrical waveguides predominantly made of silica (SiO_2) and function by guiding light along their axis through total internal reflection (TIR). These fibers consist of a core and cladding, both dielectric materials, with the core having a higher RI.[54] Silicon's integration into fiber-optic sensors significantly enhances their performance. It's highly transparent in the mid-IR spectrum, which is advantageous for temperature measurement and high-resolution sensing. For standard silica fibers, tapering is widely used to modify the dimensions to change the guiding properties of fiber, such as dispersion, nonlinearity, and modal behavior.[142] Silicon-based sensors, including dual-cavity fiber-optic pressure sensors, demonstrate remarkable sensitivity and accuracy due to their material properties. Because optical fibers are easy to modify, silica-based optical fibers have also been widely used for biological signal detection applications.[143] Innovations like embedded sensors in silicon carbide matrices and ultra-high sensitivity modulators underline silicon's pivotal role in advancing sensor technology, offering solutions for complex and harsh environments. These advancements showcase silicon's potential to create more efficient, sensitive, and robust fiber-optic sensing systems.

Kant et al.[144] researched detecting the organophosphate pesticide fenitrothion using SPR sensing technology combined with an optical fiber platform. This method features a sensing surface composed of tantalum(V) oxide (Ta_2O_5) nanoparticles within a reduced graphene oxide (rGO) matrix, enhancing the sensor's electric field and surface area, thus leading to a potent SPR signal. Such a configuration allowed for the detection of fenitrothion in varying concentrations with notable sensitivity, specificity, and speed, supporting applications in environmental monitoring through online and remote sensing.

Silicon fiber is used in pressure sensors to create highly sensitive and precise sensing devices. These sensors leverage silicon's mechanical and optical properties, integrating it with fiber-optic technology to measure pressure changes through interferometric methods and membrane deflection. They offer high resolution and minimal footprint across various applications.[145–147]

Xue Wang et al.[148] developed an all-silicon dual-cavity fiber-optic pressure sensor, notable for its ultralow pressure-temperature cross-sensitivity and capacity to endure temperatures up to 700 °C. This sensor, constructed from two silicon layers bonded directly, utilizes a sealed vacuum microcavity for pressure sensing and a silicon substrate as a secondary microcavity for temperature sensing. Its design significantly reduces the impact of thermal stress and residual pressure, making it ideal for use in harsh environments. The experiment results showed an ultralow pressure-temperature cross-sensitivity of ~5.96 Pa/°C. Therefore, the proposed fiber-optic pressure sensor provides an excellent candidate for pressure measurement in harsh and complicated environments.

Lorenzo et al.[149] fabricated one of the smallest optical fiber-facet multiplexed monolithic silicon pressure sensors designed for high sensitivity, bandwidth, and robustness suitable for turbulent airflow measurements. These fiber-facet monolithic silicon optical pressure sensors consist of a silicon diaphragm above a sealed cavity within a 125 μm wide by 5 μm thick silicon disk mounted directly onto a single-mode optical fiber

facet. These sensors, mounted on a single-mode optical fiber, offer interferometric cavities with 1.6 MHz bandwidth and high sensitivity, enabling optical multiplexing for dynamic range up to 161 kPa. This compact, high-resolution technology presents a novel alternative for turbulence measurement equipment.

The study by Lu et al.[150] introduces innovative distributed fiber optic pH sensors employing sol-gel silica-based sensitive materials, specifically silica and gold nanoparticle-enhanced silica (Au-SiO_2). These innovative sensors are created by applying these materials onto coreless fibers through a sol-gel dip-coating process. This technique allows for accurate pH monitoring in a critical range of approximately 8–12, making it especially useful for monitoring conditions in wellbore cement. The unique feature of these sensors is their enhanced sensitivity, which is achieved by either varying the thickness of the coatings or by incorporating (AuNPs) into the silica. The SiO_2 coatings have demonstrated a sensitivity of 19.9 T%/pH, while the Au-SiO_2 coatings have shown a sensitivity of 13.4 T%/pH. These sensors are characterized by their rapid response times, excellent reversibility, and stable performance under highly alkaline conditions. Notably, the (AuNPs) help to reduce corrosion seen in pure SiO_2 coatings, thereby extending the sensor's durability and reliability. This advancement marks a significant step forward in fiber optic sensor technology, highlighting its potential for widespread environmental monitoring, particularly for applications that require spatially detailed pH measurements. In this regard, Ganesh et al. comprehensively investigates the profound influence of shape, size, and geometric configurations on the plasmonic behavior of AuNPs. It highlights how variations in these parameters critically affect the surface plasmon resonance characteristics, thereby modulating the optical properties and enhancing the efficiency of plasmonic devices.[151]

Liu et al.[152] have developed a cutting-edge fiber-optic sensing platform (FOSP) utilizing a silicon Fabry-Perot interferometer (FPI) dubbed Si-FOSP. This device leverages silicon's inherent optical and thermal attributes to provide superior sensitivity and rapid response times. The Si-FOSP's design is based on the principle that variations in the optical path length (OPL) within the silicon cavity, caused by different measurands, lead to shifts in the generated interferogram. This allows for precise measurements across a range of applications. The platform benefits from the advanced state of silicon manufacturing, offering high reproducibility and cost-effectiveness. Depending on the application, Si-FOSP can be tailored as either a low-finesse or high-finesse sensor, with appropriate data demodulation techniques applied to each. Liu et al. detail the fabrication process for both versions of the Si-FOSP and demonstrate its application in three areas: as an underwater thermometer for mapping ocean thermoclines, as a flow meter for oceanic flow speed measurement, and as a bolometer for monitoring radiation from high-temperature plasma.

4. Photonic Crystal Fiber (PCF) Based SPR Biosensors

Photonic-crystal resonant technology has recently been employed for label-free cellular imaging and modeling cell-adsorption kinetics at the single-cell level with high spatial resolution through resonant wavelength-based hyperspectral imaging.[153] The optical characteristics of PCFs can further be improved to enhance the sensitivity of the optical sensors by using plasmonic materials and various lattice structures such as hexagonal, circular, square, and different core-cladding shapes. Therefore, integrating SPR sensors with PCF exhibits appealing optical characteristics and provides unique opportunities to realize SPR biosensors in a miniaturized device, which can reduce the size of the sensor significantly and improve the sensing performance.[154,155] There have been numerous PCF-based SPR sensors with different configurations and plasmonic materials as an alternative to bulky coupling configurations.[105,156–166] With its small size, single-mode operation, and capability of controlling evanescent field penetration, PCF holds great promise for improving the sensing performance of the SPR sensors. The light is guided to the sensing region through the TIR mechanism in fiber optic-based plasmonic sensors. Cladding in these structures includes a layer of noble metal as a plasmonic material and a functionalized layer of ligands and analytes to be detected. The plasmonic layer, such as metal film or nanoparticles, is usually placed on the core or in an etched cladding region. Thus far, various fiber optic-based sensors have been investigated with different configurations, including dual-core fibers.[167] D-shape fibers,[168] tapered fibers,[169,170] multi-mode fibers,[171] single-mode fibers,[172] Bragg-grating fibers,[173] and H-type fibers.[174] However, in these structures, the incident light has to pass through a narrow-angle to be directed to the sensing region. The sensors' sensing performance can be further enhanced by altering the structural parameters and designing new fiber cladding formats. In PCFs-based sensors, the cladding region consists of a periodic air-hole structure that can control incident light propagation; however, their core and cladding are similar to conventional optical fibers.[174] The TIR, photonic bandgap (PBG), or diffraction gating effects are dominant mechanisms in the PCFs to control the light propagation through modifying air holes, number of rings, or geometrical parameters of Bragg-grating structure.[175] In PCF-based SPR sensors, the metallic layer, which is the plasmonic material, can be deposited inside or outside the fiber structure. With this regard, PCF-based SPR sensors can be classified as internal or external metal layer-coated biosensors.

4.1. Internally Metal Film Coated PCF-Based SPR Biosensors

Numerous PCF-based SPR sensors have been reported in which the plasmonic metal film was coated selectively inside the air-hole surface with microscale size.[105,161,176-179] A selective silver-coated and liquid-filled modeled PCF-based SPR sensor has been shown to enhance the phase matching between the

plasmonic and core modes and improve the detection limit. It was demonstrated that selectively coating the silver layer inside the air holes improves the signal-to-noise (SNR) ratio and increases the SPR sensor's detection accuracy due to the silver's narrow-band resonance peak.[105] There have been efforts to explore other plasmonic materials for use in PCF SPR sensors as an alternative to gold and silver. For example, indium tin oxide (ITO),[180] aluminum-doped zinc oxide (AZO),[181] and titanium nitride (TiN).[182] have been studied by numerical simulations. Also, a bowl-shaped mono-core PCF SPR sensor based on titanium was used as a plasmonic material to detect cancer cells.[183] Besides, liquid-core-based PCF SPR sensors have been investigated to demonstrate positive and negative RI sensors. The designed structure consists of three layers of air holes arranged in a hexagonal format. A gold channel and six selective liquid-analyte-filled cores have been utilized to ensure the coexistence of positive and negative RI sensitivity.[159] Using FEM simulation, a maximum positive RI sensitivity of 3600 nm/RIU in the detection range of analyte RI 1.45–1.46 and a negative RI sensitivity of −5500 nm/RIU have been obtained in the operating range of 1.50–1.53. Therefore, the PCF-based SPR sensor's sensing performance can be enhanced compared to the structure entirely coated with an internal layer. In a recent study by Bing et al.,[184] a PCF-based SPR sensor was presented for urine analysis of diabetic patients where the ITO layer as the plasmonic material was coated on the polished cladding to ensure uniformity of the coating layer. The change in the RI of an analyte can be determined by analyzing the shifts in confinement loss peak. By optimizing the thickness of ITO film, the maximum wavelength sensitivity and resolution of 25000 nm/RIU and 4×10^{-6} RIU were obtained, respectively, for the RI range of 1.32–1.355.

4.2. Externally Coated Metal Film PCF-Based SPR Biosensors

The PCF-based SPR sensors with the external sensing approach have been reported to facilitate fabrication and realize the real-time detection capability. Externally gold-coated PCF sensors have been reported by many researchers.[167,185–195] For example, an externally gold-coated plasmonic biosensor based on PCF has been proposed by Rahman et al.[196] It includes two rings with a few missing holes to introduce birefringence properties and enhance the sensor's performance. Using the wavelength interrogation and the amplitude interrogation methods, a maximum wavelength sensitivity of 10,000 nm/RIU and a maximum amplitude sensitivity of 1250 RIU^{-1} with a sensor wavelength resolution of 1×10^{-5} RIU was determined. The sensor also exhibits a high figure of merit (FOM) of 260.86 RIU^{-1} for sensing biochemical liquid analytes of RI ranging from 1.33 to 1.39. In 2017, a circular lattice air-hole PCF consisting of two air-hole ring biosensors based on the SPR technique was reported by Hasan et al.[191] A thin layer of gold film as the plasmonic material is externally deposited outside the cladding region of the PCF, which facilitates the detection process as the analyte can be detected by immobilizing it onto the outer surface. Using the wavelength interrogation method, a maximum sensitivity of 2200 nm/RIU was achieved for a gold layer with a thickness of 40 nm as the RI ranges from 1.33 to 1.36. Also, a maximum sensor resolution of 3.75×10^{-5} RIU was obtained for the sensor using an amplitude interrogation method. Similarly, a PCF-based SPR biosensor has been proposed by Xudong et al.,[197] where a gold layer is coated on the external surface of the PCF. It can detect the analyte's refractive index ranging from 1.350 to 1.395 with a maximum sensitivity of 641 RIU^{-1}, a wavelength sensitivity of 11,000 nm/RIU, and a sensor resolution of 9.09×10^{-5} RIU. A facile fabrication process and high amplitude sensitivity can be obtained using eternally silver-coated PCF sensors.[43] Rifat et al.[187] A PCF plasmonic biosensor based on the external sensing mechanism where a gold film is coated on the outer layer of the cladding was also reported. Their reported maximum wavelength and amplitude sensitivity values are 4000 nm/RIU and 478 RIU^{-1}, respectively. Their proposed sensor exhibits a maximum resolution of 2.5×10^{-5} RIU for the analyte refractive index detection range, ranging from 1.33 to 1.37.

In the same way, a two-layer PCF SPR biosensor has been reported by Sujan et al.,[198] in which a gold layer with a thickness of 35 nm is coated outside the cladding structure, creating a negative real permittivity. Their design comprises a symmetric air-hole structure, and fused silica is used as the sensor's background material. Three small air holes have been utilized in the second layer and the center of the structure to enhance the coupling strength and the evanescent field. Furthermore, the missing air holes in the designed structure create a birefringence property, which improves the sensing performance of the device. By performing the wavelength interrogation and the amplitude interrogation methods, the maximum wavelength sensitivity of 9000 nm/RIU and the maximum amplitude sensitivity of 318 RIU^{-1} were obtained. The proposed sensor has also shown a maximum resolution of 1.11×10^{-5} for the analyte refractive index range of 1.34 to 1.37.

Similarly, a ring-shaped core PCF was presented by Zhou et al.[199] for practical sensing applications where a thin gold film is externally deposited on the PCF. The designed PCF uses a hexagonal lattice consisting of capillary tubes and silica rods with the same outside diameter. A ring of capillary tubes in the hexagonal lattice and two capillaries in the opposite vertices are replaced by two silica rods closest to the metal film. This can enhance the coupling strength of the evanescent field to the metal surface and create the birefringence property due to broken structural symmetry. The maximum wavelength and amplitude sensitivity of 6900 nm/RIU and 132 RIU^{-1} were obtained for the proposed sensor when the analyte's refractive index ranges from 1.33 to 1.41.

4.2.1. Biosensors Based on Plasmonic Materials

Currently, researchers are trying to utilize new plasmonic films, surpassing existing plasmonic materials, to enhance the sensor's performance. In a recent study by Hasan et al.,[200] an ultrathin niobium nanofilm is employed as a new plasmonic material on a PCF sensor. By depositing a thin aluminum oxide (Al_2O_3) film

on the outer surface of the niobium film, the coupling strength between core guided mode and SPP mode and, thus, the sensor's performance can be enhanced. Finite-element method-based analysis showed that a maximum wavelength sensitivity of 8000 nm/RIU, amplitude sensitivity of 1560 RIU^{-1}, and sensor resolution of 8.64×10^{-5} RIU can be achieved for analyte RI ranging from 1.36 to 1.40. Although the sliver offers a sharp resonance peak, it suffers oxidation in an aqueous solution. A thin film of graphene[201] or titanium dioxide[202] can be deposited on the silver layer to resolve this drawback. Also, other plasmonic materials, including ITO,[180] AZO,[181] and TiN,[182] have been investigated as an alternative to gold and silver for PCF SPR sensors. Their various structures and analyses are shown in Figure 6, respectively.

4.2.2. Multi-core PCF-based SPR biosensors

Paul et al.[186] have demonstrated a dual-core PCF-SPR biosensor where the square lattice structure was selected to increase the contact area between the core and circular gold layer. This design can enhance the energy coupling between the plasmonic and core-guided modes, improving the sensing performance of the device. Their sensor design has shown a maximum amplitude and wavelength sensitivity of 636.5 RIU^{-1} and 11,500 nm/RIU, respectively. Also, a sensor resolution of 8.7×10^{-6} RIU was obtained in the detection range of analyte RI of 1.33–1.41. Multi-core PCFs can be easily fabricated using the stack and draw technology and exhibit outstanding performance in the RI sensors.[203,204] There have been numerous plasmonic biosensors based on dual-core PCF structures. In a study reported by Wang et al.,[205] a dual-core PCF SPR biosensor based on the silver-graphene layer as a plasmonic material has been proposed with a high wavelength sensitivity of 10,000 nm/RIU and a high resolution of 1×10^{-6} RIU.

Similarly, a dual-core PCF plasmonic biosensor that has three rings of air holes has been proposed by Paul et al.[206] The first and second rings are embedded in the hexagonal lattice, and the third ring is prescribed in a circular structure, creating hybrid cladding PCF. The designed sensor employing the gold layer as the plasmonic material demonstrates a maximum wavelength sensitivity of 9000 nm/RIU and an amplitude sensitivity of 1085 RIU^{-1}. Also, a sensor resolution as high as 1.11×10^{-5} RIU is achieved for the analyte RI of 1.33–1.40.

4.2.3. D-Shaped PCF-Based SPR Biosensors

Several researchers have explored another type of PCF SPR sensor based on different cladding shapes, known as a side-polished D-shaped structure.[182,207–209] For example, Tiesheng et al.[195] reported a side-polished hexagonal lattice D-shaped PCF SPR biosensor that benefits from multiple resonances generated between fiber waveguide and plasmonic modes. Also, the coupling strength between core and surface plasmon modes can be significantly enhanced by tuning the side-polished depth and air hole size. The wavelength sensitivity of the proposed sensor was obtained as high as 21700 nm/RIU for the analyte refractive index range of 1.33–1.34. Also, a D-shaped PCF sensor based on the SPR has been demonstrated by Thenmozhi et al.,[210] where z Indium Tin oxide (ITO) is coated over the flat surface of the sensor, and the analyte is placed on top of it. The maximal spectral sensitivity of 50000 nm/RIU, a high resolution of $4x10^{-4}$ RIU, and a maximum amplitude sensitivity of 1266.67 RIU^{-1} were reported for the proposed design. Although the D-shaped PCF-based plasmonic sensor overcomes the issues associated with the uniform coating, it suffers significant confinement loss owing to the sealed top air holes.[211,212]

Furthermore, a two-sided open-channel PCF plasmonic biosensor consisting of hexagonal lattice air holes with three rings that can operate in the visible and near-infrared wavelengths has been presented by Akter et al.[213] There are four missing air holes in the second and third rings of the proposed structure to create birefringence properties and enhance the sensitivity of the PCF sensor. Using FEM simulation, the maximum reported value of amplitude and wavelength sensitivity of the device is 396 RIU^{-1} and 5000 nm/RIU, respectively. Also, a maximum sensor resolution of 2.0×10^{-5} RIU was obtained to detect analyte RI ranging from 1.33 to 1.39. Table 2 compares the sensing performance of different internally and externally coated PCF-based SPR sensors.

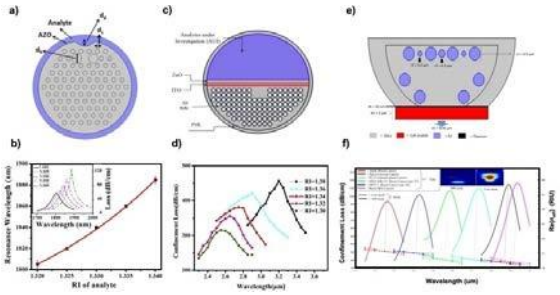

Figure 6. a) Schematic 2D view of SPR sensor b) The main graph displays the variation in resonance wavelength with the RI of the analyte. The inset illustrates the variation in confinement loss of the core mode with the RI of the analyte[181] (Reproduced with permission from Ref,[181] Copyright 2018 IEEE). c) Schematic design of the proposed D-shaped PCF-SPR sensor. d) Loss spectrum for different RI liquids ranging from RI = 1.30 to 1.38. The channel radius is 25 μm, and the thickness of the ITO and ZnO layers is 1 μm[182] (Reproduced with permission from Ref,[182] Copyright 2020 Elsevier). e) The schematic diagram illustrates a bowl-shaped SPR PCF cancer sensor with specified geometrical parameters, including the hole diameters: $r_1 = 0.5$ μm, $r_2 = 0.2$ μm, $r_3 = 0.3$ μm, and a constant pitch p = 2 μm. f) The graph depicts the mode confinement loss of X-polarization versus wavelength for various cancer cells, accompanied by the surface plasmon polariton (SPP) mode and core mode at an 80% concentration level for the proposed structure[183] (CreativeCommonsLicense4.0., with permission from 2019 IEEE).

5. Other Applications

Fiber-optic sensors, emerging as a key player in various industries, have experienced significant advancements due to progress in optics, photonics, chemistry, and biology. Their applications range from the oil and gas industry to medicine,

Table 2. Performance characteristics of internally and externally coated PCF SPR sensors.

Structure of the sensor	Plasmonic material Coating pattern	RI range	Maximum Wavelength sensitivity	Resolution or FOM	Reference	Year
Liquid analyte-filled PCF-based SPR sensor (liquid analyte in the air holes of PCF)	Internal	1.4–1.42	7040 nm/RIU	73.8 RIU^{-1}	[179]	2015
ITO-coated D-shaped PCF-based plasmonic sensor	Internal	1.22–1.33	15000 nm/RIU	6.67×10^{-6} RIU	[180]	2020
AZO-coated microchannel incorporated PCF-based SPR Sensor	Internal	1.335–1.340	5000 nm/RIU	2×10^{-5} RIU	[181]	2018
TiN-coated PCF-SPR sensor	Internal	1.385–1.40	10,000 nm/RIU	2.0×10^{-5} RIU	[214]	2019
bowl-shaped mono-core SPR sensor based on Ti-coated PCF	Internal	1.445–1.47	10 000–17 500 nm/RIU	9.33×10^{-3} RIU	[183]	2019
ITO-coated on the polished side of the PCF SPR sensor	Internal	1.320–1.355	25,000 nm/RIU	4×10^{-6} RIU	[159]	2012
SPR sensor based on PCF with selectively filled analyte channels	Internal	1.46–1.49	3000 nm/RIU	2.4×10^{-5} RIU	[215]	2015
MXene (Ti3 C2Tx) coated D-shaped PCF-based SPR-sensor	Internal	1.30–1.43	47,260 nm/RIU	2.11×10^{-6} RIU	[216]	2022
ring-shaped u-grooved selective coated PCF SPR sensor	Internal	1.29–1.40	12,500 nm/RIU	8.0×10^{-6} RIU	[217]	2023
Gold-coated dual-core with hexagonally arranged circular air holes SPR-PCF sensor	External	1.39–1.40	10,700 nm/RIU	9.34×10^{-6} RIU	[167]	2020
Three-ring hexagonal PCF- based plasmonic sensor	External	1.33–1.37	4000 nm/RIU	2.5×10^{-5} RIU	[189]	2019
Dual-polarized circular-shaped PCF -based SPR sensor with elliptical air holes	External	1.33–1.40	13,000 nm/RIU	7.69×10^{-6} RIU	[193]	2020
SPR microbiosensor based on two rings PCF with some missing holes	External	1.33–1.39	10,000 nm/RIU	1×10^{-5} RIU	[196]	2020
Gold coated two rings PCF-based SPR sensor	External	1.390–1.395	11000 nm/RIU	9.09×10^{-5} RIU	[197]	2018
hollow-core circular lattice silver-coated PCF based SPR sensor	External	1.33–1.37	4200 nm/RIU	3.33×10^{-5} RIU	[218]	2018
Dual-core Ag-TiO_2 coated PCF-based SPR sensor	External	1.29–1.39	116,000 nm/RIU	8.62×10^{-7} RIU	[202]	2019
Gold coated D-shaped PCF based SPR sensor with pure SiO_2	External	1.36–1.39	66666.67 nm/RIU	9.66×10^{-4} RIU	[207]	2020
Seven-core gold-coated PCF-based plasmonic sensor	External	1.333–1.363	1644 nm/RIU	–	[204]	2023
Three-core gold-coated PCF-based SPR sensor	External	1.37–1.42	2427 nm/RIU	4.12×10^{-5} RIU	[203]	2022
Asymmetric slotted PCF-based SPR sensor	External	1.30–1.44	1100 nm/RIU	9.09×10^{-6} RIU	[219]	2022
Dual-core silver-TiO_2 coated PCF-based SPR sensor	External	1.10–1.45	24300 nm/RIU	4.12×10^{-6} RIU	[220]	2023

environmental monitoring, and food production. The shift toward optical-fiber-based sensors is influenced by the limitations of electronic sensors, such as signal drift and electromagnetic interference, necessitating frequent calibration.[221,222] Notably, integrated with lab-on-a-chip systems, fiber optic biosensors have revolutionized the field by enabling compact, portable, and efficient sensing platforms. These integrated systems facilitate streamlined sample handling, processing, and analysis within a single device, offering simplicity in operation. Specifically, they play a crucial role in biomedicine and environmental monitoring, including detecting biomarkers in bodily fluids, monitoring patient drug levels, assessing water quality, and identifying ecological pollutants.[223]

5.1. Bioimaging

The advancements in optical fiber biosensors and their applications in biosensing and bioimaging have been a focal point of recent studies. A significant advancement in optical fiber biosensors has been the ability to perform real-time monitoring and imaging. Researchers can visualize and track biological processes and dynamics in analyte concentrations using innovations in this field, such as optical coherence tomography (OCT). As a result of these advances, complex biological phenomena can be better understood in real time.[54] These sensors offer unique advantages like compact size, immunity to electromagnetic interference, biocompatibility, and rapid response.[224] Various types of optical fiber biosensors, such as optical fiber grating, SPR, and several interferometers, have been explored. Their label-free nature enables low-cost, rapid, real-time detection with minimal analyte requirements, making them highly effective in understanding biological and pathological processes.

Lobry et al.[225] developed a D-glucose biosensor using a 35 nm thick gold layer on a tilted fiber Bragg grating (TFBG). This biosensor, enhanced with a polydopamine (PDA) layer and Concanavalin A, showcased a low LOD and high sensitivity, particularly effective in the concentration range of 10^{-6}–10^{-4} M for D-glucose. The robustness of this non-enzymatic biosensor makes it a significant advancement in glucose biosensing technology.

In a similar study by Vidal et al.,[226] TFBGs were utilized as immunosensors to detect N-terminal B-type natriuretic peptide (NT-proBNP), a biomarker for heart failure. The research explored bare and gold-coated TFBGs, focusing on different analytical methods to interpret spectral variations. They achieved remarkably low LOD–0.75 ng/mL for bare TFBG and 0.19 ng/mL for Au-coated TFBG. Their study underscores the critical impact of analytical methods in enhancing the sensitivity and reliability of biosensors, particularly in achieving lower LODs.

5.2. Quality and Analysis

In optical fiber-based sensor technology, advancements are being made that significantly impact various industries, particularly in medical and health monitoring applications. The innovative utilization of plastic optical fiber pressure sensors, as explored by Han et al.,[227] is one such example. These sensors, embedded in mattresses, can monitor sleep performance by measuring respiration and heart rate. The system leverages a specialized method to enhance pressure sensitivity and employs a two-stage amplification circuit for signal collection coupled with a unique algorithm for data processing. This comprehensive approach allows for the effective identification of various sleep-related behaviors and the precise measurement of respiratory and heart rates, showcasing the potential for home-based sleep monitoring.

In surgical settings, the differentiation between various tissues, particularly in identifying malignant tumors, is vital. Nagmeh et al.[228] have made strides in this area by developing a hybrid piezoresistive-optical-fiber sensor. This sensor combines piezoresistive force-sensing components with optical fibers to effectively detect and measure the physical properties of tissues during surgery. The dual mechanism of this sensor enhances the surgeon's ability to differentiate between tissue types and identify anomalies such as tumors, thus aiding in the precise identification of malignant tissues during surgical procedures.

Photonic crystal (PC) technologies have emerged as a powerful tool to enhance fluorescence in biosensing applications, offering unprecedented sensitivity and specificity due to their unique optical properties. These structures enhance the electromagnetic fields at the surface, thereby amplifying the fluorescence signals of biomarkers even at low concentrations.[229]

Another significant development in optical fiber technology pertains to its application in optogenetics. The rigidity and brittleness of implantable optical fibers have been a challenge, particularly for light transmission in deep brain regions of free-moving mammals. Their high Young's modulus, significantly exceeding that of neural tissue, risks tissue damage.[230] To address this, researchers like Zhang et al.[231] are exploring softer, more biocompatible, and biodegradable materials to develop tissue-friendly optical fibers. The team presented a scalable technique for manufacturing stretchable electrical and optical fiber sensors for multimodal severe deformation sensing. These sensors exhibit remarkable stretchability and durability, withstanding strains up to 580–750 % and maintaining performance through numerous stretching and bending cycles. Integrating electrical and optical detection mechanisms in these fibers enables accurate quantification of various deformations, such as bending and stretching, thereby expanding the potential applications of optical fiber technology in medical and health monitoring fields.

5.3. Food Safety

Food safety is paramount globally, and it's an area where rapid, sensitive, and affordable methods for monitoring food contaminants are continually sought. Optical biosensors, recognized for their precision in detecting various substances, including drugs, pesticides, pathogens, and heavy metals, are increasingly at the forefront of this quest. The ability of these sensors to monitor overall hygiene in the food system is particularly noteworthy.

One significant development in this field is the creation of a low-cost, portable, and reusable optical fiber-based LSPR biosensor for detecting zearalenone (ZEN) in food. This advancement, credited to Xu et al.,[55] leverages (AuNPs) and ZEN nucleic acid aptamers to achieve highly sensitive detection with a limit as low as 0.102 ng/mL. The sensor's selective nature and regenerative capability make it invaluable for on-site food safety monitoring.

Further enhancing the spectrum of optical biosensor applications, Siddharth et al.[232] developed a fiber optic-based SPR sensor integrated with MoS_2 nanosheets. This sensor stands out for its heightened sensitivity and specificity in detecting E. coli bacteria, boasting a detection limit of 94 CFU/mL. The team also tested this sensor on drinking water and orange juice samples, confirming its practicality in real-world scenarios. Their setup is shown in Figure 7.

In addition, Li et al.'s[233] research on an Ω-shaped fiber optic localized surface resonance (Ω-FOLSPR) method has opened new avenues for detecting pathogenic bacteria. This approach uses polyadenine-tailed aptamers and gold nanoparticle tags to amplify detection signals, offering flexibility in analysis time and heightened sensitivity. The sensor's ability to discern among different bacteria types enhances its practical application in bacterial detection.

Ragini et al.'s[234] work in 2023 brought forth a novel humanoid-shaped fiber optic WaveFlex biosensor. This tool is adept at rapidly detecting aflatoxin B1 (AFB1), utilizing AuNPs, GO, and multi-walled carbon nanotubes complemented by anti-AFB1 antibodies. The sensor's low DOL of 34.5 nM and its stability, selectivity, reproducibility, and reusability mark it as a significant advancement in detecting AFB1 in various food and agricultural samples. These innovations have underscored the evolving landscape of optical biosensors in ensuring food safety, highlighting their pivotal role in global health protection.

5.4. Field Environmental Monitoring

Fiber optic sensors are highly effective for environmental monitoring due to their unique properties. They easily integrate into various structures with minimal interference. They do not conduct electricity and are immune to electromagnetic and radio frequency interference. These sensors are lightweight, durable in harsh environments, and highly sensitive. They offer multiplexing for creating sensor networks and remote sensing capabilities. They can detect various parameters like strain, pressure, corrosion, temperature, and acoustic signals, making them superior to traditional electronic sensors.[235]

In the fourth industrial revolution era, the expansion of industries and the emergence of new infrastructures have intensified the need for environmental monitoring. This is particularly crucial in sectors like oil and gas and energy, where there's a demand for sensors that are resistant to electromagnetic interference and robust enough for integration into various structures. These sensors, which can be wrapped around pipes, monitor corrosion and leaks, demonstrating effective and reliable performance in such environments. A notable example is the application of Fiber Bragg Grating (FBG) sensors as a leak and corrosion detector, which was explored by Taijin et al.[236]

Rente et al.[237] developed an innovative sewer humidity monitoring system employing a polyimide-coated Fiber Bragg Grating (FBG) sensor, a portable optical sensing interrogator, and a Raspberry Pi 3 module for efficient remote data transmission. This robust system demonstrated its effectiveness in challenging environments with high corrosion rates, humidity, and hydrogen sulfide presence. It's tailored for field use, enduring long-term performance over six months with minimal maintenance, illustrating the viability of optical fiber-based sensors in harsh conditions. The data gathered correlated well with environmental temperature and precipitation, underscoring the system's accuracy and reliability for continuous environmental monitoring. The sensor is shown in Figure 8 below.

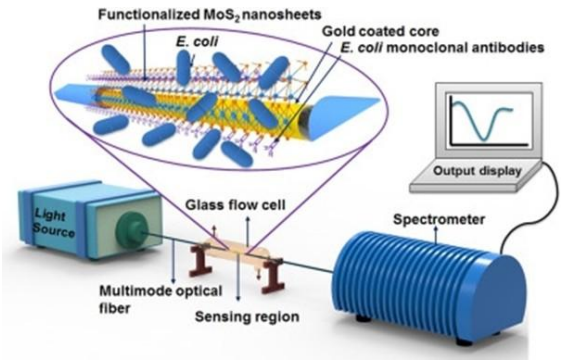

Figure 7. Schematic representation of the developed fiber optic SPR immunosensor's experimental setup for detecting E. coli[232] (Reproduced with permission from Ref,[232] Copyright 2019 ScienceDirect).

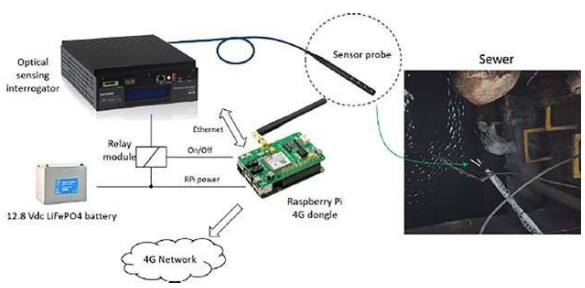

Figure 8. a) Hardware setup for the system, illustrating the sensor interrogation and data transfer approach used. b) Sensor installation at a location[237] (Reproduced with permission from Ref,[237] Copyright 2020 IEEE).

6. Future Scope and Perspectives

Future research in fiber optic biosensors, renowned for their exceptional biological performance, should focus primarily on broadening their applications. The capability to conduct real-time, label-free, specific, and highly sensitive detection using a microscopic probe is poised to revolutionize the accurate identification of biological targets. It is anticipated that forthcoming research efforts will enhance the maturity of this technology by conducting tests directly with clinical samples and under diagnostic conditions. This advancement is expected to substantially impact various applications, significantly improving outcomes in each field.

Moreover, the future of biosensor technology is poised for significant evolution across multiple disciplines, leveraging advances in materials science, nanotechnology, and computational modeling to enhance diagnostic and monitoring capabilities. Critical areas of promise include the integration of emerging materials like 2D materials, metal alloys instead of pure metals for different percentages, nano-composites, and bio-compatible materials, which can provide enhanced sensitivity, selectivity, and stability, thus broadening the utility of biosensors in harsh or clinically relevant environments. Additionally, there is a critical need for multi-analyte detection systems that can identify multiple analytes simultaneously with high precision, particularly in complex sample matrices found in environmental monitoring and clinical diagnostics.

As the demand for personalized medicine grows, developing small, power-efficient wearable and implantable biosensors that can continuously monitor health parameters or environmental exposures in real-time is becoming increasingly important. Similarly, the growing need for portable, easy-to-use biosensing devices at the point of care, especially in resource-limited settings, calls for further integration of sensor technology with wireless communication to facilitate real-time data analysis and decision-making.

Furthermore, the measurement accuracy of these biosensors can be influenced by various factors, such as pH values and temperature, which introduce measurement noise. This challenge can be addressed using optical fiber SPR biochemical sensors, which measure relevant parameters concurrently. The small size of the optical fibers allows for detecting multiple targets by individually functionalizing each fiber and then integrating them into a bundle. Multi-parameter detection can also be achieved by using different sensing materials to functionalize each core of a multi-core optical fiber. These advancements show that optical fiber sensors hold great potential in real-time multi-parameter analysis, highlighting their applicability in diverse fields, from environmental monitoring to clinical diagnostics.

7. Conclusions

This review comprehensively examines the integration of advanced plasmonic materials in PCF biosensors, highlighting significant advancements and potential future directions in biosensing technology. Through the lens of recent developments in materials science and optical engineering, it explores how graphene, transition metal dichalcogenides, black phosphorus, silicon, and germanium enhance the performance of PCF biosensors, offering improved sensitivity, specificity, and label-free detection capabilities. We delve into the principles of SPR and LSPR, crucial mechanisms underpinning the operation of these advanced biosensors. It discusses the unique properties of each plasmonic material and their impact on biosensor design and functionality, providing insights into the tailored application of these materials for enhanced biosensing performance. Reflecting on the current landscape, the review identifies critical challenges and opportunities within the field, emphasizing the importance of interdisciplinary research in overcoming obstacles and pushing the boundaries of what is possible in biosensing. It also considers the implications of these technologies for real-world applications, including medical diagnostics, environmental monitoring, and food safety, underscoring the potential of PCF biosensors to revolutionize these areas. Looking forward, the paper calls for continued innovation and collaboration across disciplines to refine further and expand the capabilities of PCF biosensors. It highlights the need for robust, scalable, and versatile biosensing platforms that can accommodate the evolving demands of healthcare, environmental science, and industry. Integrating advanced plasmonic materials within PCF structures represents a promising avenue for achieving these goals, offering a pathway to more sensitive, selective, and miniaturized sensors capable of real-time, on-site analysis. In conclusion, this review encapsulates the progress and promise of plasmonic material-integrated PCF biosensors, advocating for a future where these advanced technologies are pivotal in enhancing our ability to detect and monitor biological and environmental phenomena. By harnessing the synergies between plasmonic materials and PCF, researchers and practitioners can unlock new possibilities in biosensing, contributing to advancing science and improving society.

Acknowledgments

The authors acknowledge support from the National Science Foundation (NSF Convergence Accelerator L476) under Grant ITE-2344476 and the Bean Space Foundation.

Conflict of Interests

The authors declare no conflict of interest.

Data Availability Statement

The data that support the findings of this study are available from the corresponding author upon reasonable request.

Keywords: Optical-fiber · Surface plasmonic materials · Biosensors · Sensitivity

[1] G. K. Knopf, A. S. Bassi, Smart Biosensor Technology, 2nd ed, in CRC Press, **2018**, 3-27.
[2] D. R. Thevenot, K. Toth, R. A. Durst, G. S. Wilson, *Pure Appl. Chem.* **1999**, *71*, 2333–2348.
[3] V. S. Chaudhary, D. Kumar, S. Kumar, *IEEE Sens. J.* **2021**, *21*, 17800–17807.
[4] Z. Szittner, B. Péter, S. Kurunczi, I. Székács, R. Horváth, *Adv. Colloid Interface Sci.* **2022**, 102727.
[5] H. H. Nguyen, J. Park, S. Kang, M. Kim, *Sensors* **2015**, *15*, 10481–10510.
[6] V. Amendola, R. Pilot, M. Frasconi, O. M. Maragò, M. A. Iati, *J. Phys.: Condens. Matter* **2017**, *29*, 203002.
[7] S. Ansaryan, Y.-C. Liu, X. Li, A. M. Economou, C. S. Eberhardt, C. Jandus, H. Altug, *Nat. Biomed. Eng.* **2023**, 1–16.
[8] S. Ogawa, S. Fukushima, M. Shimatani, *Sensors* **2020**, *20*, 3563.
[9] M. J. Linman, K. Sugerman, Q. Cheng, *Sens. Actuators B Chem.* **2010**, *145*, 613–619.
[10] J. Homola, *Anal. Bioanal. Chem.* **2003**, *377*, 528–539.
[11] M. H. F. Meyer, M. Hartmann, M. Keusgen, *Biosens. Bioelectron.* **2006**, *21*, 1987–1990.
[12] Y. Li, X. Liu, Z. Lin, *Food Chem.* **2012**, *132*, 1549–1554.
[13] V. D. Krishna, K. Wu, D. Su, M. C. J. Cheeran, J.-P. Wang, A. Perez, *Food Microbiol.* **2018**, *75*, 47–54.
[14] D. R. Shankaran, K. V. Gobi, N. Miura, *Sens. Actuators B Chem.* **2007**, *121*, 158–177.
[15] D. Thacharakkal, S. Bhaskar, T. Sharma, G. Rajaraman, S. Sathish Ramamurthy, C. Subramaniam, *Chem. Eng. J.* **2024**, *480*, 148166.
[16] S. K. Mishra, S. N. Tripathi, V. Choudhary, B. D. Gupta, *Sens. Actuators B Chem.* **2014**, *199*, 190–200.
[17] P. K. Maharana, R. Jha, P. Padhy, *Sens. Actuators B Chem.* **2015**, *207*, 117–122.
[18] C. L. Wong, M. Olivo, *Plasmonics* **2014**, *9*, 809–824.
[19] D. Wang, J. F. C. Loo, J. Chen, Y. Yam, S.-C. Chen, H. He, S. K. Kong, H. P. Ho, *Sensors* **2019**, *19*, 1266.
[20] E. Hutter, J. H. Fendler, *Adv. Mater.* **2004**, *16*, 1685–1706.
[21] C. Haffner, D. Chelladurai, Y. Fedoryshyn, A. Josten, B. Baeuerle, W. Heni, T. Watanabe, T. Cui, B. Cheng, S. Saha, *Nature* **2018**, *556*, 483–486.
[22] T. Špringer, J. Homola, *Anal. Bioanal. Chem.* **2012**, *404*, 2869–2875.
[23] S. Uniyal, K. Choudhary, S. Sachdev, S. Kumar, *IEEE Sens. J.* **2022**, *22*, 11415–11426.
[24] A. Jebelli, F. Oroojalian, F. Fathi, A. Mokhtarzadeh, M. de la Guardia, *Biosens. Bioelectron.* **2020**, *169*, 112599.
[25] B. Kaur, S. Kumar, B. K. Kaushik, *IEEE Sens. J.* **2021**, *21*, 23957–23964.
[26] J. W. Chung, S. D. Kim, R. Bernhardt, J. C. Pyun, *Sens. Actuators B Chem.* **2005**, *111*, 416–422.
[27] E. Mauriz, *Sensors* **2020**, *20*, 4745.
[28] M. G. Daher, S. A. Taya, I. Colak, S. K. Patel, M. M. Olaimat, O. Ramahi, *J. Biophotonics* **2022**, *15*, e202200001.
[29] P. Sharma, P. Sharan, *IEEE Sens. J.* **2014**, *15*, 1035–1042.
[30] L. Zhang, H. Wang, H. Zhang, N. Zhang, X. Zheng, W. Li, X. Qiu, D. Yu, *Sens. Actuators B Chem.* **2022**, *369*, 132272.
[31] M. Pumera, *Mater. Today* **2011**, *14*, 308–315.
[32] X. Ge, Z. Xia, S. Guo, *Adv Funct. Mater.* **2019**, *29*, 1900318.
[33] J. Wang, M. M. Sanchez, Y. Yin, R. Herzer, L. Ma, O. G. Schmidt, *Adv. Mater. Technol.* **2020**, *5*, 1901138.
[34] Y. Zhao, S. Gan, L. Wu, J. Zhu, Y. Xiang, X. Dai, *Nanophotonics* **2020**, *9*, 327–336.
[35] Q. Ouyang, S. Zeng, L. Jiang, L. Hong, G. Xu, X.-Q. Dinh, J. Qian, S. He, J. Qu, P. Coquet, *Sci. Rep.* **2016**, *6*, 28190.
[36] A. P. Hibbins, E. Hendry, M. J. Lockyear, J. R. Sambles, *Opt. Express* **2008**, *16*, 20441–20447.
[37] R. S. Anwar, H. Ning, L. Mao, *Digital Communications and Networks* **2018**, *4*, 244–257.
[38] H. Ditlbacher, N. Galler, D. M. Koller, A. Hohenau, A. Leitner, F. R. Aussenegg, J. R. Krenn, *Opt. Express* **2008**, *16*, 10455–10464.
[39] W. Sun, Q. He, S. Sun, L. Zhou, *Light Sci. Appl.* **2016**, *5*, e16003–e16003.
[40] S.-H. Oh, H. Altug, X. Jin, T. Low, S. J. Koester, A. P. Ivanov, J. B. Edel, P. Avouris, M. S. Strano, *Nat. Commun.* **2021**, *12*, 3824.
[41] B. D. Gupta, *in Reviews in Plasmonics 2010*, Springer **2011**, 105–137.
[42] A. Hassani, M. Skorobogatiy, *Opt. Express* **2006**, *14*, 11616–11621.
[43] M. R. Momota, M. R. Hasan, *Opt. Mater. (Amst)* **2018**, *76*, 287–294.
[44] S. Heffner, J. P. Smith, *Medical and Biological Sensors and Sensor Systems Markets, Applications, and Competitors Worldwide 2nd Edition Akalorama Information Market Intelligence Report* **2006**.
[45] J. H. Banoub, R. M. Caprioli, Molecular Technologies for Detection of Chemical and Biological Agents,in Springer,**2017**, 21-51.
[46] S. E. Mowbray, A. M. Amiri, *Diagnostics* **2019**, *9*, 23.
[47] T. Pasinszki, M. Krebsz, *Adv. Clin. Chem.* **2019**, *91*, 1–29.
[48] M. E. Bosch, A. J. R. Sánchez, F. S. Rojas, C. B. Ojeda, *Sensors* **2007**, *7*, 797–859.
[49] A. B. Socorro-Leránoz, D. Santano, I. Del Villar, I. R. Matias, *Biosens. Bioelectron. X* **2019**, *1*. DOI 10.1016/j.biosx.2019.100015.
[50] N. De Acha, A. B. Socorro-Leránoz, C. Elosúa, I. R. Matías, *Biosensors* **2021**, *11*, 197.
[51] A. K. Singh, S. Mittal, M. Das, A. Saharia, M. Tiwari, *Alexandria Eng. J.* **2023**, *67*, 673–691.
[52] H. Zhang, X. Zhou, X. Li, P. Gong, Y. Zhang, Y. Zhao, *Biosensors (Basel)* **2023**, *13*. DOI: 10.3390/bios13030405.
[53] M. D. Marazuela, M. C. Moreno-Bondi, *Anal. Bioanal. Chem.* **2002**, *372*, 664–682.
[54] S. N. Khonina, N. L. Kazanskiy, M. A. Butt, *Biosensors (Basel)* **2023**, *13*. DOI 10.3390/bios13090835
[55] Y. Xu, M. Xiong, H. Yan, *Sens. Actuators B Chem.* **2021**, *336*, 129752.
[56] A. Kumar, P. Verma, P. Jindal, *Opt. Mater. (Amst)* **2022**, *128*, 112397.
[57] R. Wang, C. Liu, Y. Wei, T. Jiang, C. Liu, C. Shi, X. Zhao, L. Li, *Optik (Stuttg)* **2022**, *266*, 169603.
[58] M. Li, R. Singh, M. S. Soares, C. Marques, B. Zhang, B. Zhang, S. Kumar, S. Kumar, *Optics Express* **2022**, *30*, 13898–13914.
[59] M. Li, R. Singh, Y. Wang, C. Marques, B. Zhang, S. Kumar, *Biosensors* **2022**, *12*, 843.
[60] C. Elosua, F. J. Arregui, C. R. Zamarreño, C. Bariain, A. Luquin, M. Laguna, I. R. Matias, *Sens. Actuators B Chem.* **2012**, *173*, 523–529.
[61] P. J. Rivero, A. Urrutia, J. Goicoechea, F. J. Arregui, *Sens. Actuators B Chem.* **2012**, *173*, 244–249.
[62] S. Huang, S. U. Villafranca, I. Mehta, O. Yosfan, E. Hong, A. Wang, N. Wu, Q. Wang, S. Rao, *J. Mater. Chem. B* **2023**, *11*, 7629–7640.
[63] S. Tabassum, R. Kumar, *Adv. Mater. Technol.* **2020**, *5*, 1900792.
[64] S. Hosseinniay, A. H. Rezayan, F. Ghasemi, M. Malekmohamadi, R. A. Taheri, M. Hosseini, H. Alvandi, *Anal. Chim. Acta* **2023**, *1237*, 340580.
[65] J. Cao, T. Sun, K. T. V. Grattan, *Sens. Actuators B Chem.* **2014**, *195*, 332–351.
[66] V. Pellas, D. Hu, Y. Mazouzi, Y. Mimoun, J. Blanchard, C. Guibert, M. Salmain, S. Boujday, *Biosensors (Basel)* **2020**, *10*. DOI 10.3390/BIOS10100146.
[67] M. Loyez, E. M. Hassan, M. Lobry, F. Liu, C. Caucheteur, R. Wattiez, M. C. Derosa, W. G. Willmore, J. Albert, *ACS Sens.* **2020**, *5*, 454–463.
[68] Y. Luo, S. Hu, H. Wang, Y. Chen, J. Dong, Z. Jiang, X. Xiong, W. Zhu, W. Qiu, H. Lu, *Opt. Express* **2018**, *26*, 34250–34258.
[69] H. Zhang, X. Li, X. Zhou, P. Gong, Y. Zhao, *Opt. Lett.* **2023**, *48*, 2138–2141.
[70] D. Murugan, H. Bhatia, V. V. R. Sai, J. Satija, Transactions of the Indian National Academy of Engineering 2020, 5, 211–215.
[71] Y. Ran, J. Long, Z. Xu, Y. Yin, D. Hu, X. Long, Y. Zhang, L. Liang, H. Liang, B. O. Guan, *Biosens. Bioelectron.* **2021**, *179*, 113081.
[72] R. Sangubotla, J. Kim, *Mater. Sci. Eng., C* **2021**, *122*, 111916.
[73] F. Esposito, L. Sansone, A. Srivastava, A. M. Cusano, S. Campopiano, M. Giordano, A. Iadicicco, *Sens. Actuators B Chem.* **2021**, *347*, 130637.
[74] L. Pasquardini, N. Cennamo, G. Malleo, L. Vanzetti, L. Zeni, D. Bonamini, R. Salvia, C. Bassi, A. M. Bossi, *Sensors* **2021**, *21*, 3443.
[75] G. Li, Q. Xu, R. Singh, W. Zhang, C. Marques, Y. Xie, B. Zhang, S. Kumar, *IEEE Sens. J.* **2022**, *22*, 16904–16911.
[76] M. Lobry, M. Lobry, M. Loyez, K. Chah, E. M. Hassan, E. M. Hassan, E. Goormaghtigh, M. C. DeRosa, R. Wattiez, C. Caucheteur, *Biomed. Opt. Express* **2020**, *11*, 4862–4871.
[77] A. Rahtuvanoğlu, S. Akgönüllü, S. Karacan, A. Denizli, *ChemistrySelect* **2020**, *5*, 5683–5692.
[78] L. Zhang, Y. Tang, L. Tong, *iScience* **2020**, *23*, 100810.
[79] S. Tharani, D. Durgalakshmi, S. Balakumar, R. A. Rakkesh, *ChemistrySelect* **2022**, *7*, e202203603.
[80] O. S. Wolfbeis, *Anal. Chem.* **2008**, *80*, 4269–4283.
[81] Y. Wang, R. Singh, S. Chaudhary, B. Zhang, S. Kumar, *IEEE Trans. Instrum. Meas.* **2022**, *71*. DOI 10.1109/TIM.2022.3160536.
[82] Y. Peng, Y. Zhao, X. guang Hu, Y. Yang, *Sens. Actuators B Chem.* **2020**, *316*, 128097.
[83] H. Y. Wen, C. W. Huang, Y. Le Li, J. L. Chen, Y. T. Yeh, C. C. Chiang, *Sensors* **2020**, *20*, 1509.

[84] L. T. Ngo, W. K. Wang, Y. T. Tseng, T. C. Chang, P. L. Kuo, L. K. Chau, T. T. Huang, *Anal. Bioanal. Chem.* **2021**, *413*, 3329–3337.
[85] M. Lu, H. Zhu, L. Hong, J. Zhao, J. F. Masson, W. Peng, *ACS Appl. Mater. Interfaces* **2020**, *12*, 50929–50940.
[86] L. Li, Y. nan Zhang, W. Zheng, X. Li, Y. Zhao, *Talanta* **2022**, *247*, 123599.
[87] J. Cui, M. Zhou, Y. Li, Z. Liang, Y. Li, L. Yu, Y. Liu, Y. Liang, L. Chen, C. Yang, *Front. Cell. Infect. Microbiol.* **2021**, *11*, 665241.
[88] M. Janik, E. Brzozowska, P. Czyszczoń, A. Celebańska, M. Koba, A. Gamian, W. J. Bock, M. Śmietana, *Sens. Actuators B Chem.* **2021**, *330*, 129316.
[89] M. Chen, T. Lang, B. Cao, Y. Yu, C. Shen, *Opt. Laser Technol.* **2020**, *131*, 106445.
[90] A. Yasli, *Plasmonics* **2021**, *16*, 1605–1612.
[91] M. A. Mollah, M. Yousufali, I. M. Ankan, M. M. Rahman, H. Sarker, K. Chakrabarti, *Sens. Biosensing Res.* **2020**, *29*, 100344.
[92] K. S. Novoselov, A. K. Geim, S. V. Morozov, D. Jiang, Y. Zhang, S. V. Dubonos, I. V. Grigorieva, A. A. Firsov, *Science (1979)* **2004**, *306*, 666–669.
[93] A. A. Khorami, B. Barahimi, S. Vatani, A. S. Javanmard, *Opt. Express* **2023**, *31*, 21063–21077.
[94] N. O. Weiss, H. Zhou, L. Liao, Y. Liu, S. Jiang, Y. Huang, X. Duan, *Adv. Mater.* **2012**, *24*, 5782–5825.
[95] T. Taliercio, P. Biagioni, *Nanophotonics* **2019**, *8*, 949–990.
[96] G. V. Naik, V. M. Shalaev, A. Boltasseva, *Adv. Mater.* **2013**, *25*, 3264–3294.
[97] A. H. C. Neto, F. Guinea, N. M. R. Peres, K. S. Novoselov, A. K. Geim, *Rev. Mod. Phys.* **2009**, *81*, 109.
[98] Y.-M. Lei, M.-M. Xiao, Y.-T. Li, L. Xu, H. Zhang, Z.-Y. Zhang, G.-J. Zhang, *Biosens. Bioelectron.* **2017**, *91*, 1–7.
[99] E. Morales-Narváez, A. Merkoçi, *Adv. Mater.* **2012**, *24*, 3298–3308.
[100] Y. Shao, J. Wang, H. Wu, J. Liu, I. A. Aksay, Y. Lin, Electroanalysis **2010**, 22, 10, 1027–1036 .
[101] S. Chung, R. A. Revia, M. Zhang, *Adv. Mater.* **2021**, *33*, 1904362.
[102] Y. V. M. Reddy, J. H. Shin, V. N. Palakollu, B. Sravani, C.-H. Choi, K. Park, S.-K. Kim, G. Madhavi, J. P. Park, N. P. Shetti, *Adv. Colloid Interface Sci.* **2022**, *304*, 102664.
[103] H. Fu, S. Zhang, H. Chen, J. Weng, *IEEE Sens. J.* **2015**, *15*, 5478–5482.
[104] J. Lou, T. Cheng, S. Li, X. Zhang, *Opt. Fiber Technol.* **2019**, *50*, 206–211.
[105] A. A. Rifat, G. A. Mahdiraji, D. M. Chow, Y. G. Shee, R. Ahmed, F. R. M. Adikan, *Sensors* **2015**, *15*, 11499–11510.
[106] L. Wu, H.-S. Chu, W. S. Koh, E.-P. Li, *Opt. Express* **2010**, *18*, 14395–14400.
[107] V. Sharma, A. Kumar, S. Saharan, S. Semwal, *Plasmonics* **2023**, *18*, 1639–1649.
[108] P. Vikas, *ACS Omega* **2023**, *8*, 4627–4638.
[109] W. Zhang, R. Singh, Z. Wang, G. Li, Y. Xie, R. Jha, C. Marques, B. Zhang, S. Kumar, *Opt. Express* **2023**, *31*, 11788–11803.
[110] D. Hou, N. Luan, X. Ji, W. Zhang, Z. Zhang, X. Jiang, L. Song, Y. Qi, J. Liu, *IEEE Photonics J.* **2022**, *14*, 1–8.
[111] S. Manzeli, D. Ovchinnikov, D. Pasquier, O. V. Yazyev, A. Kis, *Nat. Rev. Mater.* **2017**, *2*, 1–15.
[112] C. M. Das, L. Kang, M. W. Chen, P. Coquet, K.-T. Yong, *ACS Appl. Nano Mater.* **2020**, *3*, 10446–10453.
[113] S. Zeng, S. Hu, J. Xia, T. Anderson, X.-Q. Dinh, X.-M. Meng, P. Coquet, K.-T. Yong, *Sens. Actuators B Chem.* **2015**, *207*, 801–810.
[114] A. Bijalwan, B. K. Singh, V. Rastogi, *Plasmonics* **2020**, *15*, 1015–1023.
[115] L. Han, X. He, L. Ge, T. Huang, H. Ding, C. Wu, *Plasmonics* **2019**, *14*, 2021–2030.
[116] N. Zhang, G. Humbert, T. Gong, P. P. Shum, K. Li, J.-L. Auguste, Z. Wu, D. J. J. Hu, F. Luan, Q. X. Dinh, *Sens. Actuators B Chem.* **2016**, *223*, 195–201.
[117] R. Verma, B. D. Gupta, R. Jha, *Sens. Actuators B Chem.* **2011**, *160*, 623–631.
[118] J. Jing, K. Liu, J. Jiang, T. Xu, S. Wang, J. Ma, Z. Zhang, W. Zhang, T. Liu,in 2021 International Conference on Optical Instruments and Technology:Micro/Nano Photonics: Materials and Devices 2022, 12283,10–15.
[119] Z. Wang, R. Singh, C. Marques, R. Jha, B. Zhang, S. Kumar, *Opt. Express* **2021**, *29*, 43793–43810.
[120] L. Li, L. Zhao, X. Zong, Y. Li, P. Li, Y. Liu, *Opt. Commun.* **2022**, *520*, 128485.
[121] C. Odac, U. Aydemir, *Res. Optics* **2021**, *3*, 100063.
[122] Q. Ouyang, S. Zeng, L. Jiang, J. Qu, X.-Q. Dinh, J. Qian, S. He, P. Coquet, K.-T. Yong, *J. Phys. Chem. C* **2017**, *121*, 6282–6289.
[123] Y. Guo, N. M. Singh, C. M. Das, Q. Ouyang, L. Kang, K. Li, P. Coquet, K.-T. Yong, *Plasmonics* **2020**, *15*, 1815–1826.
[124] X. Zhao, T. Huang, P. S. Ping, X. Wu, P. Huang, J. Pan, Y. Wu, Z. Cheng, *Sensors* **2018**, *18*, 2056.
[125] N. Ferdous, M. S. Islam, M. S. Alam, M. Y. Zamil, J. Biney, S. Vatani, J. Park, *Sci. Rep.* **2023**, *13*, 18778.
[126] W. C. Yap, Z. Yang, M. Mehboudi, J.-A. Yan, S. Barraza-Lopez, W. Zhu, *Nano Res.* **2018**, *11*, 420–430.
[127] F. Li, X. Liu, Y. Wang, Y. Li, *J. Mater. Chem. C Mater.* **2016**, *4*, 2155–2159.
[128] Y. Jia, Y. Liao, H. Cai, *Electronics (Basel)* **2022**, *11*, 332.
[129] Y. Zhang, J. Xue, W. Liu, Y. Zhang, S. Li, Z. Liu, B. Lai, J. Zhang, L. Yuan, *IEEE Sens. J.* **2022**, *22*, 4083–4089.
[130] Z. Liu, H. Chen, J. Xue, Y. Zhang, W. Liu, S. Li, Y. Zhang, B. Lai, L. Yuan, *Opt. Commun.* **2022**, *524*, 128788.
[131] Q. Zhao, J. Liu, H. Yang, H. Liu, G. Zeng, B. Huang, *Micromachines (Basel)* **2022**, *13*, 826.
[132] N. H. O. Cunha, J. P. Da Silva, *Sensors* **2022**, *22*, 3220.
[133] R. K. Gangwar, R. Min, S. Kumar, X. Li, *Front. Phys.* **2021**, *9*, 707113.
[134] L. Kou, T. Frauenheim, C. Chen, *J. Phys. Chem. Lett.* **2014**, *5*, 2675–2681.
[135] Y. Yi, Z. Sun, J. Li, P. K. Chu, X.-F. Yu, B. Y. Phosphorus Yi, Z. Sun, J. Li, X. Yu, P. K. Chu, *Small Methods* **2019**, *3*, 1900165.
[136] D. Yu, J. Li, T. Wang, X. She, Y. Sun, J. Li, L. Zhang, X.-F. Yu, D. Yang, *pss RRL* **2020**, *14*, 1900697.
[137] Y. Vasimalla, H. S. Pradhan, *JOSA B* **2022**, *39*, 324.
[138] L. Zhou, C. Liu, Z. Sun, H. Mao, L. Zhang, X. Yu, J. Zhao, X. Chen, *Biosens. Bioelectron.* **2019**, *137*, 140–147.
[139] P. Qiao, X. H. Wang, S. Gao, X. Yin, Y. Wang, P. Wang, *Biosens. Bioelectron.* **2020**, *149*, 111821.
[140] M. Ghashghaee, M. Ghambarian, *Struct. Chem.* **2019**, *30*, 85–96.
[141] P. Teng, Y. Jiang, X. Chang, Y. Shen, Z. Liu, N. Copner, J. Yang, K. Li, M. Bowkett, L. Yuan, X. Yang, *Opt. Fiber Technol.* **2021**, *66*, 102668.
[142] J. Ballato, T. Hawkins, P. Foy, R. Stolen, B. Kokuoz, M. Ellison, C. McMillen, J. Reppert, A. M. Rao, M. Daw, S. Sharma, R. Shori, O. Stafsudd, R. R. Rice, D. R. Powers, *Opt. Express* **2008**, *16*, 18675–18683.
[143] L. Novotny, B. Hecht, Principles of Nano-Optics, Cambridge University Press **2012**, 202-205.
[144] R. Kant, *Microchim. Acta* **2020**, *187*, 1–11.
[145] J. A. Dziuban, A. Gorecka-Drzazga, U. Lipowicz, *Sens. Actuators A Phys.* **1992**, *32*, 628–631.
[146] W. Wang, C. Niezrecki, X. Wang, Y. Tian, N. Wu, *Opt. Express* **2010**, *18*, 9006–9014.
[147] Y. Jiang, J. Li, Z. Zhou, X. Jiang, D. Zhang, *Sensors* **2016**, *16*, 1660.
[148] X. Wang, X. Wang, J. Jiang, J. Jiang, S. Wang, S. Wang, K. Liu, T. Liu, T. Liu, *Photon. Res.* **2021**, *9*, 521–529.
[149] S. Lorenzo, O. Solgaard, *IEEE Sens. J* **2020**, *20*, 10598–10606.
[150] F. Lu, R. Wright, P. Lu, P. C. Cvetic, P. R. Ohodnicki, *Sens. Actuators B Chem.* **2021**, *340*, 129853.
[151] K. M. Ganesh, S. Bhaskar, V. S. K. Cheerala, P. Battampara, R. Reddy, S. C. Neelakantan, N. Reddy, S. S. Ramamurthy, *Nanomater.* **2024**, *14*, 111.
[152] G. Liu, Q. Sheng, W. Hou, M. L. Reinke, M. Han, *JoVE* **2019**, *2019*, e59026.
[153] J. Juan-Colás, I. S. Hitchcock, M. Coles, S. Johnson, T. F. Krauss, in Proceedings of the National Academy of Sciences 2018, 115, 50,13204–13209.
[154] C. Liu, L. Yang, X. Lu, Q. Liu, F. Wang, J. Lv, T. Sun, H. Mu, P. K. Chu, *Opt Express* **2017**, *25*, 14227–14237.
[155] Y. Esfahani Monfared, *Plasmonics* **2020**, *15*, 535–542.
[156] B. Gauvreau, A. Hassani, M. F. Fehri, A. Kabashin, M. Skorobogatiy, *Opt. Express* **2007**, *15*, 11413–11426.
[157] A. Hassani, B. Gauvreau, M. F. Fehri, A. Kabashin, M. Skorobogatiy, *Electromagn.* **2008**, *28*, 198–213.
[158] W. Qin, S.-G. Li, J.-R. Xue, X.-J. Xin, L. Zhang, *Chin. Phys. B* **2013**, *22*, 074213.
[159] B. Shuai, L. Xia, D. Liu, *Opt. Express* **2012**, *20*, 25858–25866.
[160] M. Tian, P. Lu, L. Chen, C. Lv, D. Liu, *Opt. Commun.* **2012**, *285*, 1550–1554.
[161] J. N. Dash, R. Jha, *IEEE Photon. Technol. Lett.* **2014**, *26*, 1092–1095.
[162] A. A. Rifat, G. A. Mahdiraji, Y. M. Sua, Y. G. Shee, R. Ahmed, D. M. Chow, F. R. M. Adikan, *IEEE Photon. Technol. Lett.* **2015**, *27*, 1628–1631.
[163] L. Peng, F. Shi, G. Zhou, S. Ge, Z. Hou, C. Xia, *IEEE Photon. J.* **2015**, *7*, 1–9.
[164] F. Shi, L. Peng, G. Zhou, X. Cang, Z. Hou, C. Xia, *Plasmonics* **2015**, *10*, 1263–1268.
[165] A. K. Mishra, S. K. Mishra, B. D. Gupta, *Opt. Commun.* **2015**, *344*, 86–91.
[166] Q. Liu, S. Li, H. Chen, J. Li, Z. Fan, *Appl. Phys. Express* **2015**, *8*, 046701.
[167] A. Shafkat, *Sens. Biosensing Res.* **2020**, *28*, 100324.

[168] S.-F. Wang, M.-H. Chiu, R.-S. Chang, *Sens. Actuators B Chem.* **2006**, *114*, 120–126.
[169] M.-C. Navarrete, N. Diaz-Herrera, A. González-Cano, Ó. Esteban, *Sens Actuators B Chem.* **2014**, *190*, 881–885.
[170] Y.-C. Kim, W. Peng, S. Banerji, K. S. Booksh, *Opt. Lett.* **2005**, *30*, 2218–2220.
[171] W. Peng, S. Banerji, Y.-C. Kim, K. S. Booksh, *Opt. Lett.* **2005**, *30*, 2988–2990.
[172] A. J. C. Tubb, F. P. Payne, R. B. Millington, C. R. Lowe, *Sens. Actuators B Chem.* **1997**, *41*, 71–79.
[173] B. Špačková, J. Homola, *Opt. Express* **2009**, *17*, 23254–23264.
[174] R. A. Aoni, R. Ahmed, M. M. Alam, S. A. Razzak, *Int. J. Sci. Eng. Res* **2013**, *4*, 1–4.
[175] R. Ahmed, M. M. Khan, R. Ahmmed, A. Ahad, in OPJ, **2013**, 3, 2A, 13-19.
[176] M. F. O. Hameed, M. Y. Azab, A. M. Heikal, S. M. El-Hefnawy, S. S. A. Obayya, *IEEE Photonics Technol. Lett.* **2015**, *28*, 59–62.
[177] D. Gao, C. Guan, Y. Wen, X. Zhong, L. Yuan, *Opt. Commun.* **2014**, *313*, 94–98.
[178] W. Qin, S. Li, Y. Yao, X. Xin, J. Xue, *Opt. Lasers Eng.* **2014**, *58*, 1–8.
[179] Z. Fan, S. Li, Q. Liu, G. An, H. Chen, J. Li, D. Chao, H. Li, J. Zi, W. Tian, *IEEE Photonics J.* **2015**, *7*, 1–9.
[180] C. Liu, J. Wang, F. Wang, W. Su, L. Yang, J. Lv, G. Fu, X. Li, Q. Liu, T. Sun, *Opt. Commun.* **2020**, *464*, 125496.
[181] J. N. Dash, R. Das, R. Jha, *IEEE Photonics Technol. Lett.* **2018**, *30*, 1032–1035.
[182] V. Kaur, S. Singh, *Optik (Stuttg)* **2020**, *220*, 165135.
[183] M. A. Jabin, K. Ahmed, M. J. Rana, B. K. Paul, M. Islam, D. Vigneswaran, M. S. Uddin, *IEEE Photonics J.* **2019**, *11*, 1–10.
[184] P. Bing, J. Zhao, Q. Liu, X. Yi, Z. Li, H. Zhang, Z. Chen, J. Xu, *Eur. Phy. J. D* **2023**, *77*, 68.
[185] M. Liu, X. Yang, B. Zhao, J. Hou, P. Shum, *Mod. Phys. Lett. B* **2017**, *31*, 1750352.
[186] A. K. Paul, A. K. Sarkar, A. Khaleque, *Photonic Sens.* **2019**, *9*, 151–161.
[187] A. A. Rifat, M. R. Hasan, R. Ahmed, H. Butt, *J. Nanophotonics* **2018**, *12*, 12503.
[188] M. F. H. Arif, M. M. Hossain, N. Islam, S. M. Khaled, *Sens. Biosensing Res.* **2019**, *22*, 100252.
[189] Md. B. Hossain, Md. S. Hossain, Md. Moznuzzaman, Md. A. Hossain, Md. Tariquzzaman, Md. T. Hasan, Md. M. Rana, *J. Sens. Technol.* **2019**, *09*, 27–34.
[190] C. Liu, L. Yang, W. Su, F. Wang, T. Sun, Q. Liu, H. Mu, P. K. Chu, *Opt. Commun.* **2017**, *382*, 162–166.
[191] M. R. Hasan, S. Akter, A. A. Rifat, S. Rana, S. Ali, in Photonics, **2017**, 4, 1,18.
[192] X. Yan, B. Li, T. Cheng, S. Li, *Sensors* **2018**, *18*, 2922.
[193] M. R. Islam, A. N. M. Iftekher, K. R. Hasan, M. J. Nayen, S. Bin Islam, *Appl. Opt.* **2020**, *59*, 3296–3305.
[194] H. Thenmozhi, M. S. M. Rajan, K. Ahmed, *Optik (Stuttg)* **2019**, *180*, 264–270.
[195] T. Wu, Y. Shao, Y. Wang, S. Cao, W. Cao, F. Zhang, C. Liao, J. He, Y. Huang, M. Hou, *Opt. Express* **2017**, *25*, 20313–20322.
[196] M. M. Rahman, M. M. Rana, M. S. Anower, M. S. Rahman, A. K. Paul, *SN Appl. Sci.* **2020**, *2*, 1–11.
[197] X. Li, S. Li, X. Yan, D. Sun, Z. Liu, T. Cheng, *Micromachines (Basel)* **2018**, *9*, 640.
[198] S. Chakma, M. A. Khalek, B. K. Paul, K. Ahmed, M. R. Hasan, A. N. Bahar, *Sens. Biosensing Res.* **2018**, *18*, 7–12.
[199] X. Zhou, T. Cheng, S. Li, T. Suzuki, Y. Ohishi, *OSA Contin* **2018**, *1*, 1332–1340.
[200] M. R. Hasan, S. Akter, K. Ahmed, D. Abbott, *IEEE Photonics Technol. Lett.* **2017**, *30*, 315–318.
[201] X. Yang, Y. Lu, B. Liu, J. Yao, *Plasmonics* **2017**, *12*, 489–496.
[202] E. Haque, S. Mahmuda, M. A. Hossain, N. H. Hai, Y. Namihira, F. Ahmed, *IEEE Photonics J.* **2019**, *11*, 1–9.
[203] J. Dong, C. Zhang, S. Xia, K. Zhu, S. Zhang, Y. Yang, H. Zhu, H. Li, *Optik (Stuttg)* **2022**, *266*, 169641.
[204] H. Wang, M. Wu, S. Zheng, T. Xie, W. Dai, H. Fu, *Opt. Laser Technol.* **2023**, *164*, 109511.
[205] F. Wang, Z. Sun, C. Liu, T. Sun, P. K. Chu, *Plasmonics* **2017**, *12*, 1847–1853.
[206] A. K. Paul, A. K. Sarkar, A. B. S. Rahman, A. Khaleque, *IEEE Sens. J.* **2018**, *18*, 5761–5769.
[207] M. S. Khan, K. Ahmed, M. N. Hossain, B. K. Paul, T. K. Nguyen, V. Dhasarathan, *Optik (Stuttg)* **2020**, *202*, 163649.
[208] G. Melwin, K. Senthilnathan, *Optik (Stuttg)* **2020**, *213*, 164779.
[209] C. Liu, W. Su, Q. Liu, X. Lu, F. Wang, T. Sun, P. K. Chu, *Opt. Express* **2018**, *26*, 9039–9049.
[210] H. Thenmozhi, M. S. M. Rajan, K. Ahmed, *Optik (Stuttg)* **2019**, *180*, 264–270.
[211] D. F. Santos, A. Guerreiro, J. M. Baptista, *IEEE Sens. J.* **2015**, *15*, 5472–5477.
[212] N. Luan, R. Wang, W. Lv, J. Yao, *Opt. Express* **2015**, *23*, 8576–8582.
[213] S. Akter, M. Z. Rahman, S. Mahmud, *Results Phys.* **2019**, *13*, 102328.
[214] V. Kaur, S. Singh, *Opt. Fiber Technol.* **2019**, *48*, 159–164.
[215] A. A. Rifat, G. A. Mahdiraji, D. M. Chow, Y. G. Shee, R. Ahmed, F. R. M. Adikan, *Sensors* **2015**, *15*, 11499–11510.
[216] F. Mumtaz, M. Roman, B. Zhang, L. G. Abbas, Y. Dai, M. A. Ashraf, M. A. Fiaz, A. Kumar, *Photonics Nanostruct. Fundam. Appl.* **2022**, *52*, 101090.
[217] A. M. T. Hoque, K. F. Al-Tabatabaie, M. E. Ali, A. M. Butt, S. S. I. Mitu, K. K. Qureshi, *IEEE Access* **2023**, *11*, 74486–74499.
[218] M. R. Momota, M. R. Hasan, *Opt. Mater (Amst)* **2018**, *76*, 287–294.
[219] M. A. Rahman, T. Ahmed, M. I. Haque, M. S. Anower, *J. Sens. Technol.* **2022**, *12*, 1–17.
[220] N. Hussain, M. R. Masuk, Md. F. Hossain, A. Z. Kouzani, *Opt. Express* **2023**, *31*, 26910.
[221] M. A. Riza, Y. I. Go, S. W. Harun, R. R. J. Maier, *IEEE Sens. J.* **2020**, *20*, 7614–7627.
[222] M. Elsherif, A. E. Salih, M. G. Muñoz, F. Alam, B. AlQattan, D. S. Antonysamy, M. F. Zaki, A. K. Yetisen, S. Park, T. D. Wilkinson, H. Butt, *Adv. Photonics Res.* **2022**, *3*. DOI 10.1002/adpr.202100371.
[223] J. Cai, Y. Liu, X. Shu, *Sensors* **2023**, *23*. DOI 10.3390/s23010542.
[224] B. Li, R. Zhang, R. Bi, M. Olivo, *Biosensors* **2022**, *13*, 64.
[225] M. Lobry, D. Lahem, M. Loyez, M. Debliquy, K. Chah, M. David, C. Caucheteur, *Biosens. Bioelectron.* **2019**, *142*, 111506.
[226] M. Vidal, M. S. Soares, M. Loyez, F. M. Costa, C. Caucheteur, C. Marques, S. O. Pereira, C. Leitão, *Sensors* **2022**, *22*, 2141.
[227] P. Han, L. Li, H. Zhang, L. Guan, C. Marques, S. Savović, B. Ortega, R. Min, X. Li, *Opt. Fiber Technol.* **2021**, *64*, 102541.
[228] N. M. Bandari, R. Ahmadi, A. Hooshiar, J. Dargahi, M. Packirisamy, J. Biomed. Opt. **2017**, 22, 7, 077002.
[229] Y. Xiong, S. Shepherd, J. Tibbs, A. Bacon, W. Liu, L. D. Akin, T. Ayupova, S. Bhaskar, B. T. Cunningham, *Micromachines (Basel)* **2023**, *14*, 668.
[230] R. Nazempour, B. Zhang, Z. Ye, L. Yin, X. Lv, X. Sheng, *Adv. Fiber Mater.* **2022**, *4*, 24–42.
[231] Y. Zhang, X. Li, J. Kim, Y. Tong, E. G. Thompson, S. Jiang, Z. Feng, L. Yu, J. Wang, D. S. Ha, H. Sontheimer, B. N. Johnson, X. Jia, *Adv. Opt. Mater.* **2021**, *9*, 2001815.
[232] S. Kaushik, U. K. Tiwari, S. S. Pal, R. K. Sinha, *Biosens. Bioelectron.* **2019**, *126*, 501–509.
[233] Y. Li, X. Wang, W. Ning, E. Yang, Y. Li, Z. Luo, Y. Duan, *Biosens. Bioelectron.* **2022**, *201*, 113911.
[234] R. Singh, W. Zhang, X. Liu, B. Zhang, S. Kumar, *Biomed. Opt. Express* **2023**, *14*, 4660.
[235] K. Fidanboylu, H. Efendioğlu, in 5 Th International Advanced Technologies Symposium (IATS'09), **2009**, 6, 2-3.
[236] T. Jiang, L. Ren, Z. Jia, D. Li, H. Li, *Appl. Sci.* **2017**, *7*, 540.
[237] B. Rente, M. Fabian, Y. Chen, L. Vorreiter, H. Bustamante, T. Sun, K. T. V. Grattan, *IEEE Sens. J.* **2020**, *20*, 2976–2981.

Manuscript received: March 15, 2024